The Lichenologist (2023), **55**, 497–517
doi:10.1017/S0024282923000555

CAMBRIDGE UNIVERSITY PRESS

Standard Paper

Multi-locus phylogeny of *Bryoria* reveals recent diversification and unexpected diversity in section *Divaricatae*

Leena Myllys[1], Raquel Pino-Bodas[2], Saara Velmala[1], Li-Song Wang[3] and Trevor Goward[4]

[1]Botanical Museum, Finnish Museum of Natural History, FI-00014 University of Helsinki, Finland; [2]Area of Biodiversity and Conservation, Rey Juan Carlos University, 28933 Móstoles, Madrid, Spain; [3]Kunming Institute of Botany, Chinese Academy of Science, Heilongtan, Kunming, Yunnan, 650204, China and [4]UBC Herbarium, Beaty Museum, University of British Columbia, Vancouver, BC V6T 1Z4, Canada

Abstract

In recent years, the genus *Bryoria* (*Parmeliaceae*, *Lecanoromycetes*) has been the subject of considerable phylogenetic scrutiny. Here we used information on six gene regions, three nuclear protein-coding markers (*Mcm7*, *GAPDH* and *Tsr1*), two nuclear ribosomal markers (ITS and IGS) and a partial mitochondrial small subunit (mtSSU), to examine infrageneric relationships in the genus and to assess species delimitation in the *Bryoria bicolor*/*B. tenuis* group in section *Divaricatae*. For this purpose, phylogenetic analyses and several of the available algorithms for species delimitation (ASAP, GMYC single, GMYC multiple and bPTP) were employed. We also estimated divergence times for the genus using *BEAST. Our phylogenetic analyses based on the combined data set of six gene loci support the monophyly of sections *Americanae*, *Divaricatae* and *Implexae*, while section *Bryoria* is polyphyletic and groups in two clades. Species from *Bryoria* clade 1 are placed in an emended section *Americanae*. Our study reveals that section *Divaricatae* is young (*c.* 5 My) and is undergoing diversification, especially in South-East Asia and western North America. Separate phylogenetic analyses of section *Divaricatae* using ITS produced a topology congruent with the current species concepts. However, the remaining gene regions produced poorly resolved phylogenetic trees and the different species delimitation methods also generated highly inconsistent results, congruent with other studies that highlight the difficulty of species delimitation in groups with recent and rapid radiation. Based on our results, we describe the new species *B. ahtiana* sp. nov., characterized by its bicolorous, caespitose, widely divergent thallus, conspicuously thickening main stems, well-developed secondary branches, and rather sparse third-order branchlets. Another new lineage, referred to here as *B. tenuis* s. lat., is restricted to western North America and may represent a new species recently diverged from *B. tenuis* s. str., though further work is needed.

Keywords: fungal barcode; incomplete lineage sorting; ITS regions; lichen; species delimitation

(Accepted 5 June 2023)

Introduction

Bryoria Brodo & D. Hawksw. is a lichenized 'hair lichen' genus (*sensu* Goward *et al.* 2022) in the alectorioid clade of the *Parmeliaceae* currently including *c.* 50 accepted species (Thell *et al.* 2012). Its members are usually easily distinguished from other hair lichen genera (*Alectoria* Ach., *Nodobryoria* Common & Brodo, *Sulcaria* Bystrek, etc.) by their pale greyish to brownish or almost black thalli that are richly and finely branched and vary in habit from decumbent or erect to pendent. The genus is distributed mainly in boreal to north temperate regions of Eurasia and North America, but also occurs in the mountains of Africa, Australasia and South-East Asia (Brodo & Hawksworth 1977).

Bryoria has been divided into several sections based on thallus anatomy, chemistry and morphology (Brodo & Hawksworth 1977). Myllys *et al.* (2011) published the first comprehensive phylogeny of the genus using three gene regions (nuclear ribosomal internal transcribed spacer region (ITS), partial glyceraldehyde 3-phosphate dehydrogenase gene (*GAPDH*) and small subunit of the mitochondrial ribosomal DNA (mtSSU) and accepted the four phenotypically defined sections, namely *Bryoria*, *Divaricatae* (Du Rietz) Brodo & D. Hawksw. *Implexae* (Gyeln.) Brodo & D. Hawksw. and *Tortuosae* (Bystrek) Brodo & D. Hawksw., although the circumscription of section *Bryoria* in particular differed markedly from the original. They further introduced the monotypic section *Americanae* Myllys & Velmala for *Bryoria americana* (Motyka) Holien. Subsequent studies based on different combinations of ITS, mtSSU and partial *Mcm7* (mini-chromosome maintenance protein 7 gene) data have obtained slightly contradicting results. In Boluda *et al.* (2015) and Myllys *et al.* (2016), section *Bryoria* was recovered as polyphyletic and split into three and two monophyletic groups, respectively. Furthermore, in the phylogenies of Myllys *et al.* (2016) and Wang *et al.* (2017), section *Divaricatae* was no longer monophyletic. This was because *B. smithii* (Du Rietz) Brodo & D. Hawksw. and closely related species fell outside the section. The discrepancies between the results obtained from different phylogenies are probably explained partly by the different sampling and combination of molecular loci used and partly by implementation of different phylogenetic reconstruction methods. Nevertheless, these

Corresponding author: Leena Myllys; Email: leena.myllys@helsinki.fi

Cite this article: Myllys L, Pino-Bodas R, Velmala S, Wang L-S and Goward T (2023) Multi-locus phylogeny of *Bryoria* reveals recent diversification and unexpected diversity in section *Divaricatae*. *Lichenologist* **55**, 497–517. https://doi.org/10.1017/S0024282923000555

© The Author(s), 2023. Published by Cambridge University Press on behalf of the British Lichen Society

https://doi.org/10.1017/S0024282923000555 Published online by Cambridge University Press

studies clearly demonstrate the need for more than two or three loci to reliably resolve infrageneric relationships in this genus.

Bryoria is notorious as a taxonomically difficult genus. While phylogenetic analyses have supported the traditional circumscription of species such as *B. furcellata* (Fr.) Brodo & D. Hawksw., *B. nadvornikiana* (Gyeln.) Brodo & D. Hawksw. and *B. simplicior* (Vain.) Brodo & D. Hawksw., genetic mycobiont variation in other taxa is poorly aligned with morphological and chemical variation (Velmala *et al.* 2009, 2014; Myllys *et al.* 2011), resulting in some previously recognized 'species' being proposed for synonymy (Velmala *et al.* 2009; Boluda *et al.* 2019). The lack of correlation between genotypes and phenotypes, reported also for other lichen-forming genera, viz. *Alectoria* Ach. (McMullin *et al.* 2016), *Cladonia* P. Browne (Fontaine *et al.* 2010; Kotelko & Piercey-Normore 2010; Piercey-Normore *et al.* 2010; Pino-Bodas *et al.* 2015), *Usnea* Dill. ex Adans. (Mark *et al.* 2016) and *Xanthoparmelia* (Vain.) Hale (Leavitt *et al.* 2011), has been attributed to environmental factors (Velmala *et al.* 2009; Piercey-Normore *et al.* 2010) or differential selection pressures for morphotypes (Boluda *et al.* 2019). Spribille *et al.* (2016) suggested that basidiomycete yeast abundance in the cortex of the *B. tortuosa*/*B. fremontii* complex correlates with the chemical variation of this taxon. Recent studies have shown that molecular data are essential for assessing species boundaries in groups with high levels of phenotypic homoplasy and intraspecific morphological plasticity (Pino-Bodas *et al.* 2011, 2015; Mark *et al.* 2016). Species delimitation among closely related species with recent and rapid diversification can be especially difficult due to incomplete lineage sorting (ILS), slow mutation rates in some markers and disproportionate morphological divergence (Lumbsch & Leavitt 2011; Leavitt *et al.* 2016; Mark *et al.* 2016; Zhao *et al.* 2017; Lutsak *et al.* 2020; Jorna *et al.* 2021; Lücking *et al.* 2021; Randlane & Mark 2021).

In contrast to these findings, recent molecular studies in *Bryoria* have also revealed the existence of previously unknown lineages, resulting in the recognition of several new species based on single to three-locus phylogenies but also supported by chemistry and morphology (Jørgensen *et al.* 2012; Boluda *et al.* 2015; Myllys *et al.* 2016; Wang *et al.* 2017). The new species appear to have restricted distribution areas and are confined mainly to South-East Asia and/or western North America. Furthermore, Myllys *et al.* (2011, 2016) and McCune *et al.* (2020) reported unexpected genetic diversity in section *Divaricatae* but concluded that additional sampling was needed to test whether their samples represented cryptic species.

The main objective in the present study is to determine whether a broader sampling and the addition of further gene regions can result in a more resolved and better supported phylogeny of *Bryoria* as a whole, with particular emphasis on its diversification and infrageneric classification. At the same time, we also aim to resolve the taxonomic identity of unknown lineages discovered earlier in the *B. bicolor*/*B. tenuis* group in section *Divaricatae*. To achieve these objectives, we include additional material from South-East Asia and western North America and generate new sequences from six gene regions.

Materials and Methods

Taxon sampling

A total of 71 *Bryoria* specimens from North America, Europe and Asia were used in the molecular phylogenies (Table 1). Taxa from all five sections of *Bryoria* were included to examine infrageneric classification (see Myllys *et al.* 2016). Multiple samples from section *Divaricatae* were included to examine phylogeny and species delimitation in the *Bryoria bicolor*/*B. tenuis* group. Seven specimens, which formed a paraphyletic assemblage close to *B. bicolor* (Ehrh.) Brodo & D. Hawksw. and *B. tenuis* (E. Dahl) Brodo & D. Hawksw. but which did not group with either of the species in Myllys *et al.* (2016), were included as *Bryoria* sp. (specimens L486, L490, L678, L693, L694, L695, L696). Furthermore, an additional five specimens that did not cluster with existing taxa based on morphology and fungal ITS barcode (see Schoch *et al.* 2012) were also included in our analyses. Four of these latter specimens are new (specimens L830, L879, L880, L1038) and one (specimen L168) was used in the phylogeny of Myllys *et al.* (2011) where it was basal to the *B. bicolor*/*B. tenuis* group.

Additional herbarium specimens (ALA, CANL, H, KUN, O, TUR, UAAH and UBC) from section *Divaricatae* were examined for their morphology. These included 46 specimens filed under *B. tenuis* or *Bryoria* sp. at ALA, CANL, H, KUN, O, UAAH and UBC (Supplementary Material Table S1, available online).

Selected specimens examined for comparison. *Bryoria bicolor*. **Canada:** *British Columbia*: Queen Charlotte Islands, Moresby Island, Tasu Sound, *c.* 2 km SW of Tasu, NE slope of 'Mine Mtn', *Tsuga heterophylla-Thuja plicata-Picea sitchensis* forest (perhumid oroboreal zone), on tree, scarce, 700–800 m, 52°40′N, 132°03′W, 1980, *T. Ahti* 38973 (H H9237198).— **Finland:** *Etelä-Häme*: Janakkala, Hangastenmäki, on N-facing rock face, 9 vi 1993, *T. Kontula* s. n. (H H9216664; TLC, fumarprotocetraric and protocetraric acids; GenBank Accession no. (ITS): **OR075140**, extraction ID L140). *Etelä-Savo*: Taipalsaari, Haikkaanlahti, Vasainniemi, on NE-facing rock face at 2–2.5 m height, 61°9′N, 27°57′E, 10 x 1998, *A. Puolasmaa* s. n. (TUR 100956; GenBank Accession no. (ITS): GQ379166). *Varsinais-Suomi*: Lohja, Ojamo, Liessaari, on subinclinate N-facing granite rock face by Lohjanjärvi shore, 33–34 m, 2000, *J. Pykälä* 20134 (H H9216234; GenBank Accession no. (ITS): **OR075141**, extraction ID S316).

Bryoria fruticulosa Li S. Wang & Myllys. **China:** *Yunnan*: Lijiang Co., Laojunshan Mtn, on *Abies* sp., 4020 m, 26°37′N, 99°42′E, 2011, *L. S. Wang* & *M. Liang* 11-32088 (KUN; GenBank Accession no. (ITS): KU895855); Zhongdian Co., Geza Village, Daxueshan Mtn, on *Rhododendron* sp., 4200 m, 28°35′N, 99°51′E, 2004, *L. S. Wang* 04-23206 (KUN; GenBank Accession no. (ITS): DQ0070376 as *Bryoria* sp.). *Sichuan*: Xiangcheng Co., Daxueshan Mtn, on bushes of *Rhododendron aganniphum*, 4350 m, 28°34′N, 99°49′E, 2002, *L. S. Wang* 02-23521 (KUN—holotype).

Bryoria yunnanensis Li S. Wang & Xin Y. Wang. **China:** *Yunnan*: Dali Co., Cangshan Mtn, on branches of *Abies delavayi*, 3400 m, 25°40′N, 100°06′E, 2004, *L. S. Wang* 04–23414 (H—isotype, H9237166).

Morphology and chemistry

The specimens were tentatively identified based on morphological and chemical characters. As many *Bryoria* species tend to grow intermixed, it was often necessary to first lightly moisten the material with water. Once moist, the material was teased apart, sorted and examined for morphology under a Leica S4E StereoZoom microscope. Photographs were taken with a Nikon 810 camera equipped with an AF-S VR Micro-Nikkor 105 mm

https://doi.org/10.1017/S0024282923000555 Published online by Cambridge University Press

https://doi.org/10.1017/S0024282923000555 Published online by Cambridge University Press

Table 1. Details on taxa used in the phylogenetic analyses, including voucher information and GenBank Accession numbers. New species and sequences are in bold.

Taxon	Voucher specimen and DNA extraction ID	Locality	ITS	IGS	mtSSU	*Mcm*7	*GAPDH*	*Tsr*1
Bryocaulon divergens	*Talbot* & *Myers* UNI062-34 (H), L475	USA, Alaska	KJ947935	**OR060783**	KR995314	KJ948013	KJ947979	KP888173
***Bryoria ahtiana* sp. nov.**	*Hermansson* 12625 (UPS), L168	Russia, Komi Republic	HQ402693	**OR060815**	HQ402647	**OR060732**	HQ402614	**OR060769**
***B. ahtiana* sp. nov.**	*McCune* et al. 36219 (H, OSC), L880	USA, Alaska	MN906272	**OR060816**	–	–	–	–
B. alaskana	*Dillman* 10 v 11:5 (UBC), L404	USA, Alaska	KJ947955	**OR060790**	–	KJ948079	–	**OR060748**
B. americana	*Goward* 02-165 (UBC), L199	Canada, British Columbia	HQ402678	**OR060786**	HQ402637	KJ948016	HQ402606	**OR060747**
B. asiatica	*Wang* et al. 15-49748 (KUN), L780	China, Yunnan	**OR075125**	**OR060807**	**OR075168**	**OR060728**	**OR060705**	**OR060768**
B. barbata	*Wang* 14-44036 (H, KUN), L776	China, Yunnan	**OR075126**	**OR060806**	**OR075167**	–	–	–
B. bicolor	*Hermansson* 14110 (UPS), L156	Sweden, Dalarna	HQ402692	**OR060833**	HQ402646	**OR060739**	HQ402613	**OR060779**
B. bicolor	*Velmala* 24 et al. (H), S23	Finland, Koillismaa	HQ402689	**OR060834**	HQ402644	KJ948019	HQ417113	**OR060780**
B. bicolor	*Kuusinen* 1063 & *Lampinen* (H), L183	Finland, Etelä-Häme	HQ402691	-	HQ402645	KJ948018	HQ402612	**OR060781**
B. bicolor	*Björk* 42900 (UBC), L811	USA, Alaska	**OR075127**	**OR060835**	–	**OR060740**	**OR060721**	-
B. bicolor	*Tarasova* s. n. (H), L576	Russia, Archangelsk Region	**OR075128**	-	–	**OR060738**	**OR060720**	-
B. bicolor	*McCune* 39526 (H), L1039	Canada, British Columbia	**OR075129**	**OR060832**	**OR075184**	**OR060737**	**OR060719**	-
B. bicolor	*McCune* 39506 (H), L1040	Canada, British Columbia	**OR075130**	**OR060831**	**OR075183**	**OR060736**	**OR060718**	-
B. capillaris	*Haikonen* 22228 (H), L141	Finland, Etelä-Häme	FJ668493	FJ668455	FJ668427	KJ948020	FJ668399	**OR060761**
B. carlottae	*Dillman* 20 viii 12:4 (UBC), L611	USA, Alaska	KX158214	**OR060794**	**OR075155**	KX158241	–	–
B. confusa	*Wang* 06-26974 (KUN), S292	China, Yunnan	HQ402686	–	-	KJ948024	HQ417112	–
B. confusa	*Wang* 15-49720 (KUN), L786	China, Yunnan	–	–	**OR100726**	–	–	–
B. divergescens	*Wang* 06-26244 (KUN), S284	China, Yunnan	HQ402705	**OR060788**	HQ402654	KJ948025	–	–
B. fastigiata	*Wang* et al. 06-26696 (KUN), S288	China, Yunnan	HQ402706	**OR060789**	HQ402655	KJ948026	–	–
B. fremontii	*Velmala* et al. 13b (H), S13	Finland, Koillismaa	FJ668498	FJ668460	FJ668432	KJ948029	FJ668404	**OR060746**
B. friabilis	*Dillman* 11 v 11:6 (UBC), L407	USA, Alaska	KJ396435	KJ396492	**OR075162**	**OR060725**	KJ954308	**OR060760**
B. fruticulosa	*Wang* 13-38482 (KUN), L788	China, Yunnan	**OR075139**	**OR060814**	–	–	–	–
B. fruticulosa	*Wang* et al. 06-26700 (KUN), S291	China, Yunnan	HQ402702	**OR060813**	HQ402651	–	HQ402618	–
B. fruticulosa	*Wang* 09-30973 (KUN)	China, Yunnan	KU895854	–	–	–	–	–
B. furcellata	*Haikonen* 22770 (H), L147	Finland, Etelä-Savo	HQ402722	KJ396494	HQ402667	KJ948031	HQ402627	**OR060749**
B. fuscescens	*Velmala* 51 & *Halonen* (H), S56	Finland, Koillismaa	GQ996291	KJ396502	GQ996332	KJ948035	GQ996263	**OR060762**
B. glabra	*Halonen* s. n. (OULU), L186	Finland, Koillismaa	FJ668494	FJ668456	FJ668428	KJ948036	FJ668400	**OR060756**

(*Continued*)

https://doi.org/10.1017/S0024282923000555 Published online by Cambridge University Press

Table 1. (*Continued*)

Taxon	Voucher specimen and DNA extraction ID	Locality	ITS	IGS	mtSSU	*Mcm7*	*GAPDH*	*Tsr*1
B. hengduanensis	*Wang* et al. 06-26692 (KUN), S287	China, Yunnan	HQ402704	**OR060787**	HQ402653	KJ948038	–	–
B. himalayensis	*Wang* et al. 15-49750 (KUN), L791	China, Yunnan	**OR075131**	**OR060791**	**OR075154**	**OR060722**	–	–
B. implexa	*Urbanavichus* 05-1270 (KPABG), S168	Russia, Murmansk Region	KJ396448	KJ396521	**OR075163**	KR857214	KJ954320	**OR060764**
B. inactiva	*Goward* 12-02 (UBC), L400b	Canada, British Columbia	**OR075132**	**OR060803**	**OR075161**	**OR060724**	**OR060702**	**OR060759**
B. indonesica	*Wedin* 4058 (UPS), L172	New Zealand, Gisborne	HQ402688	–	–	–	–	–
B. irwinii	*Dillman* 10 viii 11:3 (UBC), L411	USA, Alaska	KJ947953	**OR060798**	**OR075157**	KJ948077	**OR060701**	**OR060753**
B. kockiana (psoromic acid chemotype)	*Nossov* 20019-1 (UBC), L394	USA, Alaska	KJ396453	**OR060804**	**OR075164**	KX158255	**OR060703**	**OR060765**
B. kockiana (acid-deficient chemotype)	*Jovan* 4 viii 11-18 (UBC), L630	USA, Alaska	**OR075133**	**OR060805**	**OR075165**	**OR060726**	**OR060704**	**OR060766**
B. kuemmerleana	*Sohrabi* 4656 (H), L244a	Iran, East-Azarbaijan	GQ996295	KJ396531	GQ996324	KJ948042	GQ996267	**OR060763**
B. lactinea	*Wang* 06-26966 (KUN), S279	China, Yunnan	HQ402699	**OR060792**	–	KJ948050	–	–
B. nadvornikiana	*Hollinger* 1859 (UBC), L371	USA, North Carolina	KR857116	**OR060800**	**OR075158**	KR857198	KR857158	**OR060755**
B. nepalensis	*Wang* 13-38203 (KUN)	China, Yunnan	KU895874	–	–	–	–	–
B. nitidula	*Granbo* s. n. (UPS), L163	Sweden, Ångermanland	HQ402713	**OR060797**	HQ402658	KJ948054	HQ402620	**OR060752**
B. perspinosa	*Wang* et al. 06-26547 (KUN), S296	China, Yunnan	HQ402698	**OR060793**	–	–	–	–
B. pikei	*Björk* 21120 (UBC), L369	USA, Oregon	KJ947938	**OR060802**	**OR075160**	KJ948023	KJ947982	**OR060758**
B. poeltii	*Wang* et al. 06-26697 (KUN), S295	China, Yunnan	HQ402701	**OR060799**	HQ402650	KJ948057	HQ402617	**OR060754**
B. pseudofuscescens	*Goward* 06-1066a (UBC), L379a	Canada, British Columbia	KJ947942	**OR060801**	**OR075159**	KJ948043	KJ947985	**OR060757**
B. rigida	*Wang* 06-26208 (KUN), S289	China, Yunnan	HQ402703	**OR060809**	HQ402652	KJ948061	–	–
B. rigida	*Wang* 14-43962 (KUN), L798	China, Yunnan	KU895880	**OR060810**	**OR075170**	**OR060729**	–	–
B. rigida	*Wang* et al. 14-46052 (KUN), L796	China, Yunnan	**OR075134**	**OR060812**	-	**OR060731**	–	–
B. rigida	*Wang* et al. 14-44100 (KUN), L797	China, Yunnan	**OR075135**	**OR060811**	-	**OR060730**	–	–
B. simplicior	*Ahti* 61399 (H), L231b	Russia, Sakha Republic	HQ402716	**OR060795**	HQ402661	KJ948062	HQ402601	**OR060750**
B. smithii	*Velmala* et al. 60 (H), S65	Finland, Varsinais-Suomi	HQ402684	-	HQ402642	KJ948065	HQ402609	**OR060767**
B. smithii	*Tibell* 23319 (UPS), L174	India, Uttaranchal	HQ402685	-	HQ402610	KJ948064	HQ402643	-
B. tenuis	*Dillman* 2013:258 (UBC), L692	USA, Alaska	KX158201	**OR060817**	**OR075171**	KX158228	**OR060706**	**OR060770**
B. tenuis	*Velmala* et al. 64 (H), S70	Finland, Kainuu,	HQ402694	**OR060818**	HQ402648	KJ948074	HQ402615	**OR060771**
B. tenuis	*Hermansson* 12855d (UPS), L164	Sweden, Dalarna	HQ402695	-	HQ402649	KJ948073	HQ402616	-
B. tenuis	*Dillman* 2010-31 (UBC), L412	USA, Alaska	**OR075136**	**OR060819**	**OR075172**	**OR060733**	**OR060707**	-

(*Continued*)

https://doi.org/10.1017/S0024282923000555 Published online by Cambridge University Press

Table 1. (*Continued*)

Taxon	Voucher specimen and DNA extraction ID	Locality	ITS	IGS	mtSSU	*Mcm7*	*GAPDH*	*Tsr*1
B. tenuis	*Dillman* 2013:259 (UBC), L681	USA, Alaska	KX158200	**OR060820**	**OR075173**	KX158227	**OR060708**	**OR060772**
B. tenuis s. lat.	*Ahti* 70083 & *Talbot* (H), L486	USA, Alaska	KX158202	**OR060821**	**OR075174**	KX158229	**OR060709**	**OR060773**
B. tenuis s. lat.	*Talbot* & *Myers* UNI062-34A (H), L490	USA, Alaska	KX158203	**OR060823**	**OR075175**	KX158230	**OR060710**	**OR060774**
B. tenuis s. lat.	*Björk* 32228 (UBC), L693	Canada, British Columbia	KX158207	**OR060824**	**OR075176**	KX158234	**OR060711**	**OR060775**
B. tenuis s. lat.	*Björk* 29881 (UBC), L694	Canada, British Columbia	KX158208	**OR060828**	**OR075180**	KX158235	**OR075180**	-
B. tenuis s. lat.	*Björk* 29879 (UBC), L695	Canada, British Columbia	KX158206	**OR060826**	**OR075178**	KX158233	**OR060713**	**OR060777**
B. tenuis s. lat.	*Dillman* 2012:44 (UBC), L696	USA, Alaska	KX158205	**OR060825**	**OR075177**	KX158232	**OR060712**	**OR060776**
B. tenuis s. lat.	*Rielly* 21 vi 2016: 8 (UBC), L830	USA, Alaska	**OR075143**	**OR060827**	**OR075179**	**OR060734**	**OR060714**	-
B. tenuis s. lat.	*Björk* 29740 (UBC), L678	Canada, British Columbia	KX158204	**OR060829**	**OR075181**	KX158231	**OR060716**	-
B. tenuis s. lat	*McCune* 36039 et al. (H, OSC), L879	USA, Alaska	MN906266	**OR060822**	-	–	-	-
B. tenuis s. lat.	*McCune* 39535 (H), L1038	Canada, British Columbia	**OR075138**	**OR060830**	**OR075182**	**OR060735**	**OR060717**	**OR060778**
B. trichodes	*Launis* 661216 (H), L464	USA, Maine	**OR075137**	**OR060796**	**OR075156**	**OR060723**	**OR060700**	**OR060751**
B. variabilis	*Wang* 04-23184 (KUN), S286	China, Yunnan	HQ402683	–	–	–	–	–
B. vrangiana	*Velmala* et al. 43a (H), S45	Finland, Koillismaa	GQ996302	KJ396568	GQ996328	KJ948048	GQ996275	–
B. wui	*Wang* 13-38467 (KUN), L778	China, Yunnan	KU895887	–	**OR075166**	**OR060727**	–	–
B. yunnanensis	*Wang* 13-38784 (KUN), L802	China, Yunnan	KU895888	**OR060808**	**OR075169**	–	–	–
B. yunnanensis	*Wang* 10-31501 (KUN)	China, Yunnan	KU895889	–	–	–	–	–
Gowardia arctica	*Pajunen* s. n. (OULU), S146	Russia, Nenetsia	EU282503	**OR060784**	**OR075152**	KJ948082	EU282519	**OR060742**
Nodobryoria abbreviata	*Knudsen* 1305 (H), L152	USA, California	HQ402675	–	HQ402634	KJ948085	KJ947991	**OR060743**
N. oregana	*Goward* 05-26 (UBC), L198a	Canada, British Columbia	KJ947959	–	**OR075153**	KJ948087	KJ947992	**OR060744**
Pseudephebe pubescens	*Ahti* 63704 (H), L221	USA, Alaska	HQ402676	**OR060785**	HQ402635	KJ948091	HQ402604	**OR060745**
Usnea dasopoga	*Myllys* 080413-4 (H), L523	Finland, Uusimaa	KJ947975	**OR060782**	–	KJ948104	KJ948002	**OR060741**

f/2.8 G IF-ED lens (Nikon, Japan), and attached to a Kaiser 5510: RS 1 camera stand with RA1 camera arm (Kaiser Fototechnik, Germany). Serial images were taken with digiCamControl (© 2014 Duka Istvan; http://digicamcontrol.com/), and stacked to a single image using Zerene Stacker (Zerene Systems, USA).

Secondary compound metabolites were studied using K (10% potassium hydroxide) and Pd (1,4-phenylenediamine) spot tests and with thin-layer chromatography (TLC) using solvents A and B (Orange *et al.* 2001).

Molecular methods

Six markers (three ribosomal RNA-coding and three low-copy protein-coding) were used to infer the *Bryoria* phylogenies: 1) complete (*c.* 0.5 kb) ITS regions; 2) *c.* 0.4 kb region from the intergenic spacer of the nuclear rDNA (IGS); 3) *c.* 1 kb region from the mtSSU gene; 4) *c.* 0.6 kb region from the *Mcm7* gene; 5) *c.* 1 kb from the *GAPDH* gene spanning three exons and three introns; 6) *c.* 0.6 kb region from the ribosome biogenesis protein (*Tsr*1). The first five markers were selected based on our previous studies of the genus *Bryoria* (i.e. Velmala *et al.* 2009, 2014; Myllys *et al.* 2011, 2014, 2016). The *Tsr*1 region has been shown to have potential in resolving clades at both higher and lower taxonomic levels within the *Parmeliaceae* (Divakar *et al.* 2015; Widhelm *et al.* 2016).

Total DNA was extracted from a fragment of each thallus *c.* 0·5–4 cm long using the DNeasy Blood & Tissue Kit (Qiagen, Maryland, USA) as described in Myllys *et al.* (2011). Specimens were extracted from the same material already used for the TLC analysis to avoid possible contamination from mixed collections. Polymerase chain reactions (PCRs) were prepared using PuReTaq Ready-To-Go PCR Beads (GE Healthcare, Chicago, Illinois, USA). Each 25 µl reaction volume contained 19–21 µl distilled water (dH_2O), 1 µl of each primer (10 µM), and 2–4 µl extracted DNA. The annealing temperatures and primers used for amplification and sequencing are given in Table 2.

PCR products were purified and sequenced by Macrogen Inc. (Amsterdam, The Netherlands; www.macrogen.com), or, alternatively, cleaned with ExoSAP (Affymetrix, Santa Clara, California, USA) and sequenced by FIMM Genomics (https://www2.helsinki.fi/en/infrastructures/genome-analysis/infrastructures/fimm-genomics). The resulting contig sequences of each specimen were assembled using the program Sequencher v. 5.1. (Gene Codes Corp., Ann Arbor, Michigan, USA).

Phylogenetic analyses

Our first aim in this study was to examine the infrageneric structure of the genus. For this we used specimens for which at least three gene regions out of six had been sequenced, since specimens with fewer gene regions have missing data and can potentially result in too few informative characters for clade support (Wiens 2006). One sample of each species or chemotype was selected except for section *Divaricatae* for which we included all available candidate specimens. The data set included 63 ingroup specimens. *Usnea dasopoga* (Ach.) Nyl. was used as an outgroup taxon and *Gowardia arctica* Halonen *et al.*, *Nodobryoria abbreviata* (Müll. Arg.) Common & Brodo, *N. oregana* (Tuck.) Common & Brodo and *Pseudephebe pubescens* (L.) M. Choisy were included to confirm the monophyly of the ingroup.

To examine the phylogeny and species delimitation within the *B. bicolor*/*B. tenuis* group in section *Divaricatae*, we performed a separate analysis using a standard DNA barcode for fungi (i.e. ITS regions) (see Schoch *et al.* 2012), including all 42 available sequences of this section (see Table 1). *Bryoria americana* was used as an outgroup taxon based on the phylogenies by Myllys

Table 2. Primers and annealing conditions used for the PCR and sequencing.

Gene locus	Primer	Primer sequence (5'–3')	Annealing temp. (°C)	Reference
GAPDH	Gpd1-LM	ATT GGC CGC ATC GTC TTC CGC AA	54–56	Myllys *et al.* 2002
	Gpd2-LM	CCC ACT CGT TGT CGT ACC A	54–56	Myllys *et al.* 2002
IGS	IGS12B	CTG GGG GTC AAC TGA AG	50–55	Printzen & Ekman 2002
	SSU72R	TTG CTT AAA CTT AGA CAT G	50–55	Gargas & Taylor 1992
	IGSf	TAG TGG CCG WTR GCT ATC ATT	50–52	Wirtz *et al.* 2008
	IGSr	TGC ATG GCT TAA TCT TTG AG	50–52	Wirtz *et al.* 2008
ITS	ITS1-F	CTT GGT CAT TTA GAG GAA GTA A	56–60	Gardes & Bruns 1993
	ITS4	TCC TCC GCT TAT TGA TAT GC	56–60	White *et al.* 1990
	ITS1-LM	GAA CCT GCG GAA GGA TCA TT	56–60	Myllys *et al.* 1999
	ITS2-KL	ATG CTT AAG TTC AGC GGG TA	56–60	Lohtander *et al.* 1998
Mcm7	x.Mcm7.f	CGT ACA CYT GTG ATC GAT GTG	56	Leavitt *et al.* 2011
	Mcm7.1348R	GAY TTD GCI ACI CCI GGR TCW CCC AT	56	Schmitt *et al.* 2009
mtSSU	mtSSU1-KL	AGT GGT GTA CAG GTG AGT A	50–52	Lohtander *et al.* 2002
	mtSSU2-KL	ATG TGG CAC GTC TAT AGC CCA	50–52	Lohtander *et al.* 2002
	mrSSU1	AGC AGT GAG GAA TAT TGG TC	56–62	Zoller *et al.* 1999
	mrSSU3R	ATG TGG CAC GTC TAT AGC CC	56–62	Zoller *et al.* 1999
*Tsr*1	Tsr1-ParmF	GAG ATT GAG CTT CAT CCT AAT GGC T	56	Divakar *et al.* 2015
	Tsr1-ParmR	ACA GCT GCA GAG CCT TGA ACC ACT	56	Divakar *et al.* 2015

https://doi.org/10.1017/S0024282923000555 Published online by Cambridge University Press

et al. (2011, 2016). For comparison, the following *Divaricatae* data sets were analyzed from the remaining five gene loci using all the available sequences: 1) IGS data set with 30 ingroup specimens; 2) mtSSU data set with 30 ingroup specimens; 3) *GAPDH* data set with 27 ingroup specimens; 4) *Mcm7* data set with 31 ingroup specimens; 5) *Tsr*1 data set with 15 ingroup specimens. Gene regions were aligned separately with MUSCLE v. 3.8.31 (Edgar 2004) using EMBL-EBI's freely available web service (http://www.ebi.ac.uk/Tools/msa/muscle/). The alignments have been deposited in Dryad (https://doi.org/10.5061/dryad.6djh9w15w).

For all seven data sets, we performed maximum parsimony, maximum likelihood and Bayesian analyses. Parsimony analyses were performed in TNT v. 1.1 for Windows (Goloboff *et al.* 2008) using the option 'Traditional Search' with the following settings: random addition of sequences with 100 replicates and TBR branch swapping algorithm. Ten trees were saved for each replicate. The bootstrapping method as implemented in TNT was used with 1000 replicates to estimate node support. Maximum likelihood analyses were performed with RAxML v. 8.1.15 (Stamatakis 2014) on the CSC-IT Center for Science server (https://www.csc.fi/). We divided the data set into 23 partitions: ITS1, 5.8S, ITS2, IGS, mtSSU, each three codon positions of *Mcm7*, *GAPDH* and *Tsr*1, and introns of *GAPDH*. These partitions were analyzed under the universal GTR-GAMMA model. Node support was estimated with 1000 bootstrap replicates using the rapid bootstrap algorithm.

For the Bayesian analyses, the optimal substitution model for each locus was calculated in jModelTest (Posada 2008), using the Akaike information criterion (AIC). The models selected were: TrNef + G for ITS1, IGS, *GAPDH*; JC for 5.8S; K80 + G for ITS2; TrNef + I + G for *Mcm7*; SYM + I + G for mtSSU; SYM + G for *Tsr*1. The Bayesian analyses were run in MrBayes v. 3.2.6 (Ronquist *et al.* 2012) on the CIPRES Science Gateway v. 3.1 (Miller *et al.* 2010). For the concatenated analysis, 23 partitions were considered and the models selected by jModelTest were used. The posterior probabilities were approximated by sampling trees using Markov chain Monte Carlo (MCMC). Two simultaneous runs with 20 000 000 generations each, starting with a random tree and employing four simultaneous chains, were executed. Every 1000th tree was saved into a file. The first 25% of trees was deleted as burn-in. Convergence between chains was assessed in Tracer v. 1.7 (Rambaut *et al.* 2018), plotting the likelihood versus generation number and the average standard deviation of split frequencies (≤ 0.01). Branches with posterior probabilities ≥ 0.95 and bootstrap values ≥ 70% were considered strongly supported.

Dating analyses

Due to the absence of *Bryoria* fossils, the divergence time of *Bryoria* was inferred using the substitution rate for ITS (3.4×10^{-3} subst./site/my) described for *Melanohalea* (Leavitt *et al.* 2012) following Boluda *et al.* (2019). The analyses were implemented in *BEAST considering unlinking clock and tree models for each locus, using the GTR + G substitution model for each partition, a strict clock, Yule process, a piecewise linear and constant root. Two runs of 100 000 000 generations, sampled every 1000 generations, were executed. The convergence was assessed with ESS. LogCombiner was used to merge the runs after removing 10% of generations as burn-in. The tree was summarized with TreeAnnotator v. 1.8 (Rambaut & Drummond 2013) using the maximum clade credibility tree option for the target tree type.

Species delimitation analyses

Following an integrative taxonomy approach (Will *et al.* 2005; Padial *et al.* 2009), we used several delimitation methods to assess species boundaries in section *Divaricatae* and compared the results with those from morphological data. Firstly, we used species delimitation methods without *a priori* information. By comparing the results of these with the phenotypic variation observed in the group, the most plausible species hypotheses were evaluated with a validation method (Bayes Factor), which requires the assignment of specimens to putative species.

We used three different prediction methods to assess species boundaries in section *Divaricatae*: 1) Assemble Species by Automatic Partitioning (ASAP) (Puillandre *et al.* 2021), 2) the Poisson Tree Processes (bPTP) method (Zhang *et al.* 2013) and 3) the General Mixed Yule Coalescent (GMYC) method (Pons *et al.* 2006). ASAP is a method based on pairwise genetic distances from single-locus sequence alignment (Puillandre *et al.* 2021) to identify the transition between intraspecific and interspecific genetic variation, and bPTP is a model that infers putative species boundaries on a given phylogenetic input tree (Zhang *et al.* 2013). GMYC is similar to bPTP but requires an ultrametric tree as input (Fujisawa & Barraclough 2013; Zhang *et al.* 2013). None of the methods require a prior hypothesis of the putative number of species used. Due to the low number of available sequences for *Tsr*1, species delimitation analyses were not conducted for this locus.

The outgroup was removed in order to improve the delimitation results. The online version of ASAP (https://bioinfo.mnhn.fr/abi/public/asap/#) was used. The analyses were implemented with three distance models (JC69, K80, p-distances). bPTP was run on the bPTP web server (https://species.h-its.org/ptp/) using the trees from the ML analyses as input. MCMC was run for 100 000 generations, using default values for the other parameters.

ML trees for each locus were transformed into ultrametric trees using the *ape* package (Paradis *et al.* 2004) and used as input for the GMYC analyses. GMYC was run with the *splits* package (http://r-forge.r-project.org/projects/splits/), using single and multiple thresholds.

*BEAST (Heled & Drummond 2010) implemented in BEAST v. 1.8 (Drummond *et al.* 2012) was used to calculate marginal likelihoods with the Path Sampling and Stepping-Stone sampling algorithms, under a strict clock for each locus, Yule process model and constant population size. The MCMC chain was run for 50 000 000 generations and 100 steps. The different species delimitation hypotheses generated by different species delimitation methods were compared using Bayes Factor, calculated as 2× (marginal likelihood Model 1 – marginal likelihood Model 2). The hypotheses tested are listed below and in Table 3. Hypotheses 1 and 2 follow the current taxonomy and species concept used in this study and hypotheses 3–12 are obtained from species delimitation analyses. Species hypotheses that considered an unrealistic number of species (≥ 20 species) were not tested.

Hypothesis 1: current circumscription of the species with *B. tenuis* and *B. tenuis* s. lat. as separate species (14 species).

Hypothesis 2: current circumscription of the species but *B. tenuis* and *B. tenuis* s. lat. conspecific (13 species).

Hypothesis 3: hypothesis generated by ASAP for ITS, *GAPDH* and *Mcm7* (two species; we tested if subclade I and subclade II represent two separate species).

Hypothesis 4: hypothesis generated by bPTP for *GAPDH* (three species; we tested if *B. asiatica* (Du Rietz) Brodo & D. Hawksw is a

https://doi.org/10.1017/S0024282923000555 Published online by Cambridge University Press

Table 3. Results obtained from species delimitation analyses in section *Divaricatae*. ah = *B. ahtiana*, as = *B. asiatica*, ba = *B. barbata*, bi = *B. bicolor*, co = *B. confusa*, fr = *B. fruticulosa*, in = *B. indonesica*, ne = *B. nepalensis*, ri = *B. rigida*, sm = *B. smithii*, te = *B. tenuis*, tl = *B. tenuis* s. lat., va = *B. variabilis*, wu = *B. wui*, yu = *B. yunnanensis*. Numbers before colon represent putative species delimited by each method. Letter and number combinations after species refer to specimen IDs. Species delimitations consistent with the current species concepts in *Divaricatae* subclade II are shown in bold. Hypothesis numbers 3 to 12 marked in the Table correspond to those tested using Bayes factor (see text and Table 5 for details).

Method	ITS	IGS	mtSSU	*GAPDH*	*Mcm7*
ASAP	2: (co, in, ne, sm, va, wu) + (ah, as, ba, bi, fr, ri, te, tl, yu) Hypothesis 3	2: **ba** + (as, bi, fr, ri, te, ah, tl) 10: **as** + **ba** + **ri** + (ah, fr, yu) + (biS23, biL811, biL1039, biL1040) + biL156 + (teS70, teL412) + (teL692, teL681) + (tlL681, tlL486, tlL490, tlL693, tlL695, tlL696, tlL830, tlL678, tlL1038) + (tlL879, tlL694)	4: (co, sm, wu) + **ri** + (ah, bi, te, tl, yu) + (ba, as) Hypothesis 8	2: (co, sm) + (ah, as, bi, fr, te, tl) Hypothesis 3	2: (co, sm, wu) + (ah, as, ba, bi, ri, te, tl, yu) Hypothesis 3
GMYC single	28: co + in + ne + sm + va + wu + **as** + **ba** + ahL880 + ahL168 + biL1040 + (biL156, biL1039, biL811, biS23) + (biL576, biL183) + frL788 + frS291 + (riS289, riL798) + riL796 + riL797 + teL692 + teL681 + teL164 + teL412 + teS70 + (tlL695, tlL1038, tlL490, tlL693, tlL696, tlL486, tlL830) + tlL694 + tlL879 + yuL802 + yuKU	25: **as** + **ba** + ahL168 + (ahL880, yuL802) + biL156 + (biS23, biL811) + biL1039 + biL1040 + frS291 + frL788 + riS289 + riL796 + riL796 + riL797 + teL681 + teL692 + teS70 + teL412 + tlL694 + tlL879 + (tlL830, tlL696) + tlL1038 + tlL490 + (tlL486, tlL695, tlL693) + tlL676	4: (co, smS65) + (smL174, wu) + (ah, bi, ri, te, tl, yu) + (as, ba) Hypothesis 5	11: co + smS65 + smL174 + **ah** + **as** + **fr** + (biL156, biL183, biL1039, L1040) + (biL576, biL811, biS23) + (tlL678, tlL694, tlL695, teL692, teS70) + (tlL486, tlL490, tlL693, tlL696, tlL1038, teL164, teL412, teL681) + tlL830 Hypothesis 10	27: co + smS65 (smL174, wu) + **as** + biL183 + biS23 + biL811 + (biL156, biL576, biL1040) + riL796 + riL797 + riL798 + riS289 + teL412 + teS70 + teL681 + teL164 + teL692 + (tlL486, tlL490) + tlL1038 + tlL830 + tlL830 + tlL1039 + tlL695 + tlL693 + tlL696 + tlL694 + tlL678
GMYC multiple	23: in + (co, sm, wu) + (ne, va) + **ah** + **as** + **ba** + biL1040 + (biL156, biL1039, biL811, biS23) + (biL576, biL183) + frL788 + frS291 + frKU + (riS289, riL798) + (riL796, Li797) + teL692 + teL681 + teL164 + (teL412, teS70) + (tlL695, tlL1038, tlL490, tlL693, tlL696, tlL486, tlL830) + tl879 + tlL694 + yuL802 + yuKU	21: **as** + **ba** + ahL168 + (ahL880, yu) + biL156 + (biS23, biL811) + biL1039 + biL1040 + frS291 + frL788 + riS289 + riL798 + riL796 + riL797 + (teL681, teL682) + teS70 + teL412 + tlL694 + tlL879 + (tlL830, tlL695, tlL1038, tlL490, tlL486, tlL695, tlL693) + tlL678	20: co + wu + smL174 + smS65 + **as** + **ba** + **yu** + (ah, bi) + riS291 + riL798 + tlS291 + tlL678 + tlL694 + tlL693 + teL164 + (tlL490, tlL695) + (tlL486, teL412, teS70, tlL696) + (teL681, tlL830) + teL692 + tlL1038	13: co + **fr** + smL174 + smS65 + **ah** + **as** + (biL156, biL183, biL1039, biL1040) + (biL576, biL811, biS23) + (teL412, teL164) + (teL681, tlL486, tlL490, tlL496, tlL693, tlL696) + (teL692, teS70, tlL678, tlL694, tlL695) + tlL830 + tlL1038 Hypothesis 12	20: (co, smS65) + (smL174, wu) + **as** + (ah, biL156, biL1040) + biL183 + biS23 + riL796 + riL797 + riL798 + riS289 + biL811 + (biL183, teL412, teS70) + teL681 + teL164 + (tlL486, tlL490, tlL1038) + tlL830 + (tlL695, tlL693) + tlL696 + (tlL694, tlL692) + tlL678
bPTP	12: co + sm + wu + (va, ne) + **as** + **ba** + in + **ri** + **te** + **yu** + (bi, fr) + (ah, tl) Hypothesis 11	4: as + **ba** + **ri** + (ah, bi, fr, te, tl, yu) Hypothesis 6	5: (co, sm, wu) + (ah, bi, te, tl, yu) + (as, ba) + riL798 + riS289 Hypothesis 9	3: (co, sm) + **as** + (ah, bi, fr, te, tl) Hypothesis 4	4: (co, sm, wu) + **ah** + (as, biL183, biL811, biL1039, biS23, ri, te, tl) + (biL156, biL576, biL1040) Hypothesis 7

separate species in subclade II and if *B. smithii* in subclade I is not a distinct species).

Hypothesis 5: hypothesis generated by GMYC single for mtSSU (four species; we tested if *B. asiatica* and *B. barbata* Li S. Wang & Dong Liu are conspecific and the remaining species in subclade II form a separate species).

Hypothesis 6: hypothesis generated by bPTP for IGS (four species; we tested if *B. asiatica*, *B. barbata* and *B. rigida* P. M. Jørg. & Myllys are distinct species in subclade II).

Hypothesis 7: hypothesis generated by bPTP for *Mcm7* (four species; we tested if *B. confusa* (D. D. Awasthi) Brodo & D. Hawksw., *B. smithii* and *B. wui* Li S. Wang in subclade I are conspecific, and if *B. ahtiana* sp. nov. is an independent species in subclade II).

Hypothesis 8: hypothesis generated by ASAP for mtSSU (four species; we tested if *B. rigida* is a distinct species, if *B. asiatica* and *B. barbata* in subclade II are conspecific and if *B. confusa*, *B. smithii* and *B. wui* in subclade I are conspecific).

Hypothesis 9: hypothesis generated by bPTP for mtSSU (five species; same as hypothesis 8 but *B. rigida* is divided into two species).

Hypothesis 10: hypothesis generated by GMYC single for *GAPDH* (11 species; we tested if *B. ahtiana*, *B. asiatica*, *B. confusa* and *B. fruticulosa* are all distinct species, if *B. bicolor* and *B. smithii* both represent two separate species and if *B. tenuis* and *B. tenuis* s. lat. are divided into three separate species, two of which contain specimens of both taxa).

Hypothesis 11: hypothesis generated by bPTP for ITS (12 species; we tested if *B. asiatica*, *B. barbata*, *B. confusa*, *B. indonesica* (P. M. Jørg.) Brodo & D. Hawksw., *B. rigida*, *B. smithii*, *B. tenuis*, *B. wui* and *B. yunnanensis* are all distinct species, if *B. bicolor* and *B. fruticulosa* are conspecific, if *B. ahtiana* and *B. tenuis* s. lat. are conspecific and if

https://doi.org/10.1017/S0024282923000555 Published online by Cambridge University Press

B. variabilis (Bystrek) Brodo & D. Hawksw. and *B. nepalensis* D. D. Awasthi are conspecific).

Hypothesis 12: hypothesis generated by GMYC multiple for *GAPDH* (13 species; we tested if *B. ahtiana*, *B. asiatica*, *B. confusa* and *B. fruticulosa* are all good species, if both *B. bicolor* and *B. smithii* are divided into two species and if *B. tenuis* and *B. tenuis* s. lat. are divided into five separate species, two of which contain specimens of both taxa).

Results

We generated 190 new sequences for this study: 20 ITS (including four sequences obtained from additional specimens), 54 IGS, 34 mtSSU, 19 *Mcm*7, 22 *GAPDH* and 41 *Tsr*1 sequences. The aligned data matrix contained 521 aligned nucleotide position characters in ITS, 440 in IGS, 657 in mtSSU, 987 in *GAPDH*, 587 in *Mcm*7, and 597 in *Tsr*1. The final alignment of the six-locus concatenated data set was 3789 positions in length, with 416 phylogenetically informative characters. Of these variable characters, 62 occurred in the ITS region, 80 in the IGS, 33 in the mtSSU, 50 in the *Mcm*7, 96 in the *GAPDH* and 95 in the *Tsr*1. The ITS *Divaricatae* data matrix included 502 characters, of which 86 (17%) were phylogenetically informative within the ingroup. The IGS data set included 423 characters, of which 36 (9%) were informative, the mtSSU data set 645/21 (3%) characters, the *GAPDH* data set 987/59 (6%), the *Mcm*7 data set 587/43 (7%) and the *Tsr*1 data set 597/34 (6%) characters. The overall amount of missing data in the genus phylogeny was *c*. 16%; the largest amount was in the *Tsr*1 and *GAPDH* data sets (40% and 25%, respectively), whereas ITS data were complete. Since the topologies of the Bayesian and maximum likelihood analyses did not show any strongly supported conflicts, only the trees obtained from the Bayesian analyses are shown (Figs 1 & 2). Maximum parsimony analyses yielded slightly differing results in section *Divaricatae* and are presented separately (Supplementary Material Figs S1 and S2, available online). The results obtained from parsimony analyses are discussed only if they conflicted with the phylogenies obtained from Bayesian and ML analyses.

Six-locus phylogeny of the genus Bryoria

Overall, the analyses of the six-locus data set resulted in highly resolved phylogenies and strongly supported clades (Fig. 1). Section *Bryoria sensu* Myllys *et al.* (2011) was recovered as polyphyletic and divided into two strongly supported groups. The first group (referred to here as *Bryoria* clade 1) includes *B. alaskana* Myllys & Goward, *B. carlottae* Brodo & D. Hawksw., *B. divergescens* (Nyl.) Brodo & D. Hawksw., *B. fastigiata* Li S. Wang & H. Harada, *B. hengduanensis* Li S. Wang & H. Harada, *B. himalayensis* (Motyka) Brodo & D. Hawksw., *B. lactinea* (Nyl.) Brodo & D. Hawksw. and *B. perspinosa* (Bystrek) Brodo & D. Hawksw., and was resolved as sister to *B. americana* with high confidence (PP = 1 in Bayesian analysis/100% in ML analysis). Section *Tortuosae*, consisting of *B. fremontii* (Tuck.) Brodo & D. Hawksw. only, appears as basal to this clade, although the relationship remains poorly supported (0.82/55%); it is chemically unique in the genus, containing the pulvinic acid derivative vulpinic acid. The second group of section *Bryoria* (*Bryoria* clade 2, supported by 1/99%), consisting of *B. furcellata*, *B. irwinii* Goward & Myllys, *B. nadvornikiana*, *B. nitidula* (Th. Fr.) Brodo & D. Hawksw., *B. poeltii* (Bystrek) Brodo & D. Hawksw., *B. simplicior* and *B. trichodes* (Michx.) Brodo & D. Hawksw., clustered with strongly supported (1/100%) section *Implexae* with high confidence (1/99%).

Section *Divaricatae* as defined in Myllys *et al.* (2011) was recovered as monophyletic (0.99/86%) and consists of two strongly supported lineages, referred to here as subclades I and II. Subclade I includes *B. confusa*, *B. smithii* and *B. wui*, while subclade II encompasses *B. asiatica* (represented by one specimen), *B. barbata* (one specimen), *B. bicolor*, *B. fruticulosa* (one specimen), *B. rigida*, *B. yunnanensis* (one specimen) and one specimen collected on the Komi Peninsula in Russia (*Bryoria* sp. L168), with *B. asiatica* and *B. barbata* resolved as basal. *Bryoria rigida* (four specimens) and *Bryoria bicolor* (seven specimens) were both resolved as strongly supported lineages. *Bryoria tenuis* (five specimens) was not resolved as monophyletic, but grouped instead with eight North American *Bryoria* sp. specimens, referred to here as *B. tenuis* s. lat. This group was strongly supported in the Bayesian analysis (0.97) but poorly supported in the ML analysis (53%). In the parsimony analysis, *B. bicolor* and *B. tenuis* s. str. were not resolved as monophyletic but instead appeared in a poorly supported polytomy with single specimens of *B. fruticulosa* and *B. yunnanensis* together with eight *B. tenuis* s. lat. specimens (Supplementary Material Fig. S1).

Divergence time of Bryoria

Figure 3 shows the dating results of the genus *Bryoria*. Only the ages of supported clades are discussed. Our results indicate that *Bryoria* diverged 11.5 Mya (9.58-13.71 Mya) during the Miocene. Subclade I of *Divaricatae*, consisting of *B. confusa*, *B. smithii* and *B. wui*, did not form a monophyletic clade with the other species of the section. It originated 1.35 Mya (0.73–2.03 Mya), while the remaining *Divaricatae* species diverged sometime in the last 5 My: *B. asiatica* and *B. barbata* diverged 2.3 Mya (0.32–3.88 Mya), while *B. tenuis* s. str. and *B. tenuis* s. lat. were the most recent to diverge 0.31 Mya (0.08–0.55 Mya).

Single gene phylogenies of section Divaricatae

Based on the separate analysis of the ITS data set, subclade I is strongly supported (1/100%) and nested within paraphyletic subclade II (Fig. 2). *Bryoria indonesica*, *B. nepalensis* and *B. variabilis* are included in subclade I in addition to *B. confusa*, *B. smithii* and *B. wui*. In the parsimony analysis, the two subclades were both resolved as monophyletic (Supplementary Material Fig. S2, available online). In subclade II, the ITS sequence of a collection from Alaska (L880) was recovered in a strongly supported clade (1/95%) with the Komi Peninsula specimen (L168). This lineage is described below as the new species *B. ahtiana* (Fig. 4A, Table 4). All the currently recognized morphospecies represented by multiple samples were recovered as monophyletic and strongly supported in subclade II. The Chinese species *B. fruticulosa* and *B. yunnanensis* represented by three and two samples, respectively, formed monophyletic groups with high confidence (1/89% and 0.98/92%). *Bryoria fruticulosa* specimens typically have twisted and fragile third-order branchlets which are lacking in other species in this complex, while the two *B. yunnanensis* specimens have distinct main branches, lack third-order branchlets and are fertile (Fig. 4C & D, Table 4) (Wang *et al.* 2017). Seven *B. bicolor* specimens collected from various parts of the world (Canada, Finland, Russia, Sweden and the USA) formed a strongly supported group (0.97/85%) (Fig. 2). All specimens share the typical morphology of *B. bicolor* characterized by an

https://doi.org/10.1017/S0024282923000555 Published online by Cambridge University Press

Figure 1. Phylogeny of *Bryoria* based on six gene loci (*GAPDH*, ITS, IGS, *Mcm*7, mtSSU and *Tsr*1) resulting from the Bayesian analysis (−Lnl = 1.883884e + 04). This is a 50% majority-rule consensus tree. Posterior probabilities obtained from the Bayesian analysis and maximum likelihood bootstrap values obtained from the ML analysis are shown at nodes. In section *Divaricatae*, strongly supported infraspecific nodes are indicated with a circle for clarity. In colour online.

erect growth form without distinct main branches, abundant second- and third-order branches and branchlets arising at right angles (Fig. 4B, Table 4). Likewise, five *B. tenuis* specimens collected in Alaska, USA, Finland and Sweden group together with high confidence (1/99%) (Fig. 2). Ten *B. tenuis* s. lat. specimens, all collected in western Canada and Alaska, form a monophyletic group within subclade II, separate from *B. tenuis* s. str (Fig. 2). In the Bayesian analysis, the clade was poorly supported, and in the ML analysis it was moderately strongly supported. The morphology of *B. tenuis* (including *B. tenuis* s. lat.) is discussed in more detail below, in the section 'Morphology of *Bryoria tenuis*'.

The number of specimens included in other single gene analyses was generally lower than in the ITS analyses and therefore the results are not directly comparable (Fig. 2). *Bryoria rigida*

https://doi.org/10.1017/S0024282923000555 Published online by Cambridge University Press

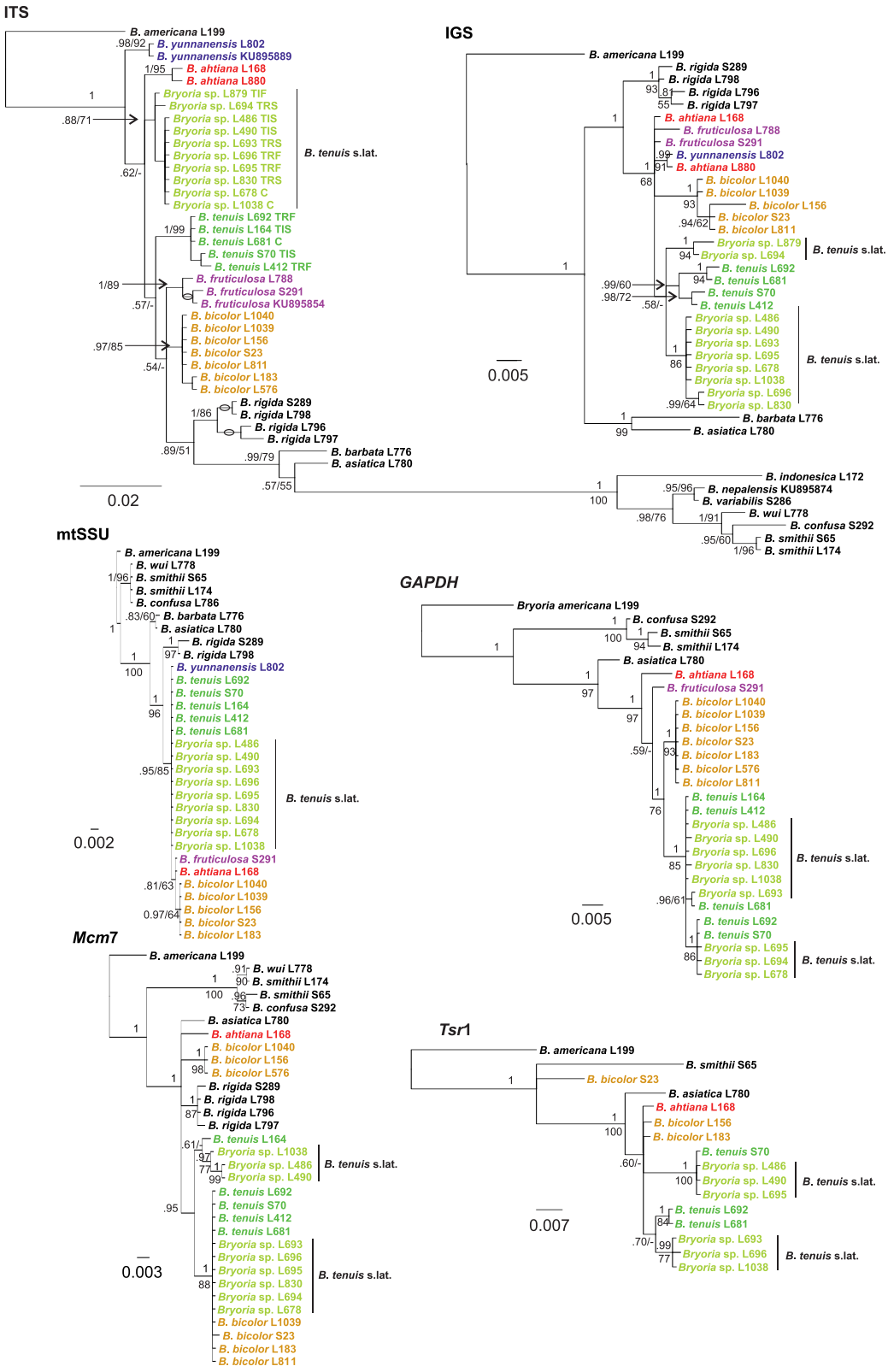

Figure 2. Single-locus *Divaricatae* phylogenies obtained from the Bayesian analyses (−Lnl value obtained from *GAPDH* analysis = 2.243487e + 03; IGS = 1.171037e + 03; ITS = 1.802841e + 03; *Mcm7* = 1.341538e + 03; mtSSU = 1.158121e + 03; *Tsr*1 = 1.493921e + 03). These are 50% majority-rule consensus trees. Posterior probabilities obtained from the Bayesian analysis and maximum likelihood bootstrap values obtained from the ML analysis are shown at nodes. Morphotypes of *Bryoria tenuis* s. str. and *B. tenuis* s. lat. are indicated for each specimen in the ITS phylogeny: C = cobwebby, TIF = thickening-flexuose, TIS = thickening-spinulose, TRF = thread-flexuose, TRS = thread-spinulose; see also Fig. 5. Strongly supported infraspecific nodes in the ITS phylogeny are indicated with an open circle for clarity.

https://doi.org/10.1017/S0024282923000555 Published online by Cambridge University Press

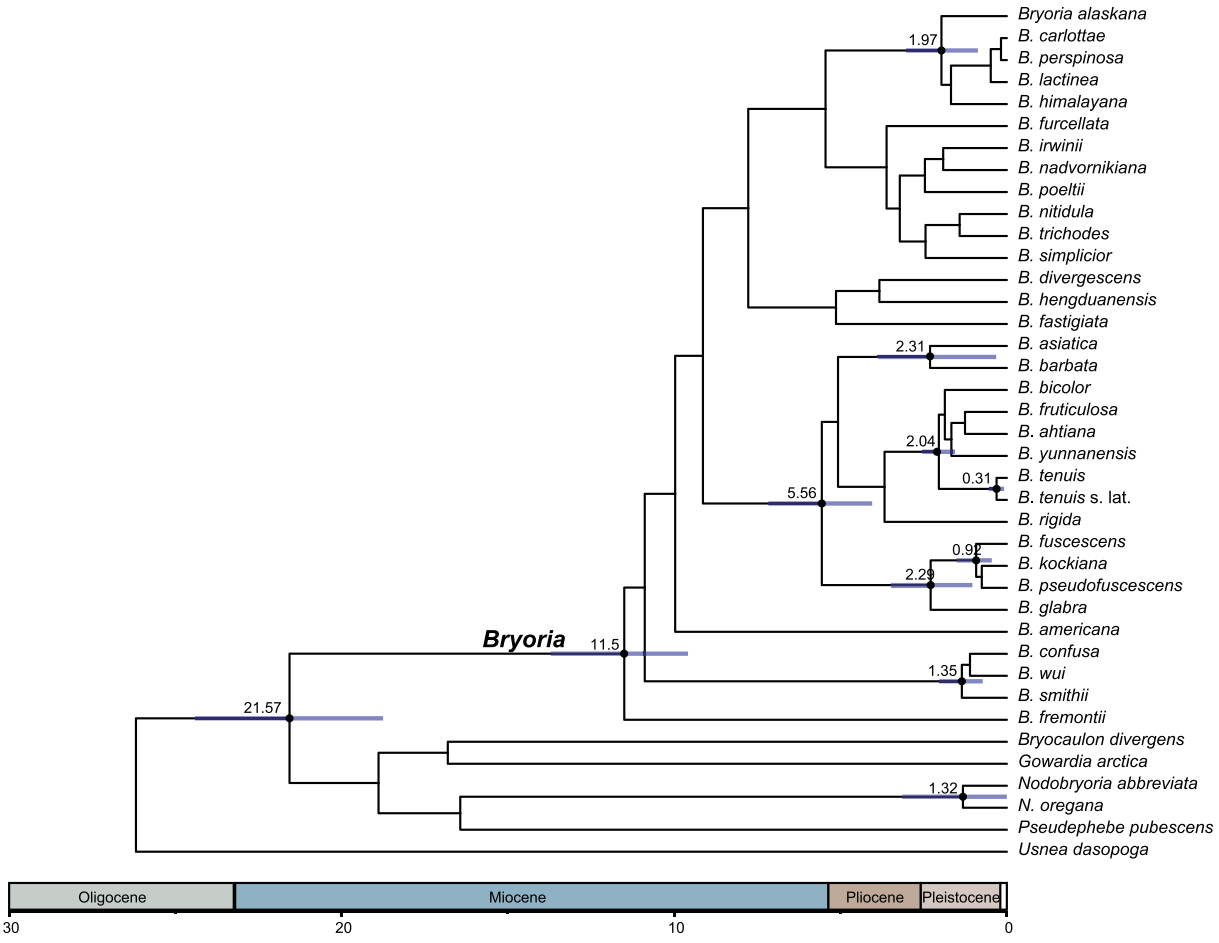

Figure 3. Phylogeny of *Bryoria* based on six loci as implemented in *BEAST. Nodes with posterior probability (PP) ≥ 0.95 support are indicated with a black dot. Mean age (million years) of the node and bars, showing the 95% highest posterior density (HPD) interval, are indicated on supported branches. In colour online.

was strongly supported in all analyses (absent from the *GAPDH* and *Tsr*1 phylogenies) but otherwise resolution within subclade II often remained low and in some cases conflicted with the results obtained from ITS data. The IGS phylogeny mostly agrees with the results obtained from the ITS data: *B. bicolor* and *B. tenuis* s. str. were both monophyletic and *B. tenuis* s. lat. specimens were divided into two strongly supported groups. *Bryoria ahtiana* was not resolved as monophyletic since specimen L880 grouped with a single specimen of *B. yunnanensis* (0.99/91%) and specimen L168 was placed outside of this group. In the mtSSU phylogeny, *B. bicolor* was resolved as monophyletic (0.97/64%) and nested in a group containing all *B. ahtiana, B. fruticulosa*, *B. tenuis*, *B. tenuis* s. lat. and *B. yunnanensis* specimens; otherwise, relationships within this group remain unresolved. In the *GAPDH* phylogeny, *B. bicolor* was monophyletic and strongly supported (1/93%). *Bryoria tenuis* and *B. tenuis* s. lat. specimens clustered together with strong support (1/85%). The tree obtained from the *Mcm7* data was inconsistent with the results obtained from ITS data: the monophyly of *B. bicolor* was not recovered as four specimens grouped instead with four *B. tenuis* and six *B. tenuis* s. lat. specimens in an unresolved polytomy with high confidence. One *B. tenuis*, three *B. bicolor* and three *B. tenuis* s. lat. specimens were left outside of this group. In the *Tsr*1 phylogeny, one *B. bicolor* specimen (S23) was placed outside of the strongly supported clade, which includes two *B. bicolor* specimens and single specimens of *B. asiatica* and *B. ahtiana* in addition to three *B. tenuis* and six *B. tenuis* s. lat. specimens. Within this group, two specimens representing *B. tenuis* formed a strongly supported clade and one *B. tenuis* specimen grouped with three *B. tenuis* s. lat. specimens with high confidence (1/100%).

Morphology of Bryoria tenuis

We examined the morphology of all specimens of *B. tenuis* s. str. and *B. tenuis* s. lat. included in our phylogenies, as well as material available at several herbaria (altogether 62 specimens) (Supplementary Material Table S1, available online). According to our results, *B. tenuis* appears to be a highly phenotypically plastic species, as illustrated in Fig. 5. Much of this plasticity is accounted for by variation in the main stems, which can be cobwebby (i.e. finely threadlike) and pliant (i.e. easily flexed) throughout (Fig. 5A), threadlike and pliant throughout (Fig. 5B), or else thickened and brittle in older parts (Fig. 5C). Also variable are the third-order branchlets which, as assessed in the terminal portions of the main stems, vary from short and rather stiff (Fig. 5B & C) to longer and more flexuous (Fig. 5D), with the latter state often correlated with a tendency for the main stems to weakly arc in their terminal portions (e.g. Fig. 5E). Taking these traits in combination results in five broadly defined, and possibly to some extent intergrading, thallus morphologies: cobwebby (Fig. 5A), threadlike-spinulose (Fig. 5B), threadlike-flexuose (Fig. 5E), thickening-spinulose (Fig. 5C), and thickening-flexuose (Fig. 5D).

https://doi.org/10.1017/S0024282923000555 Published online by Cambridge University Press

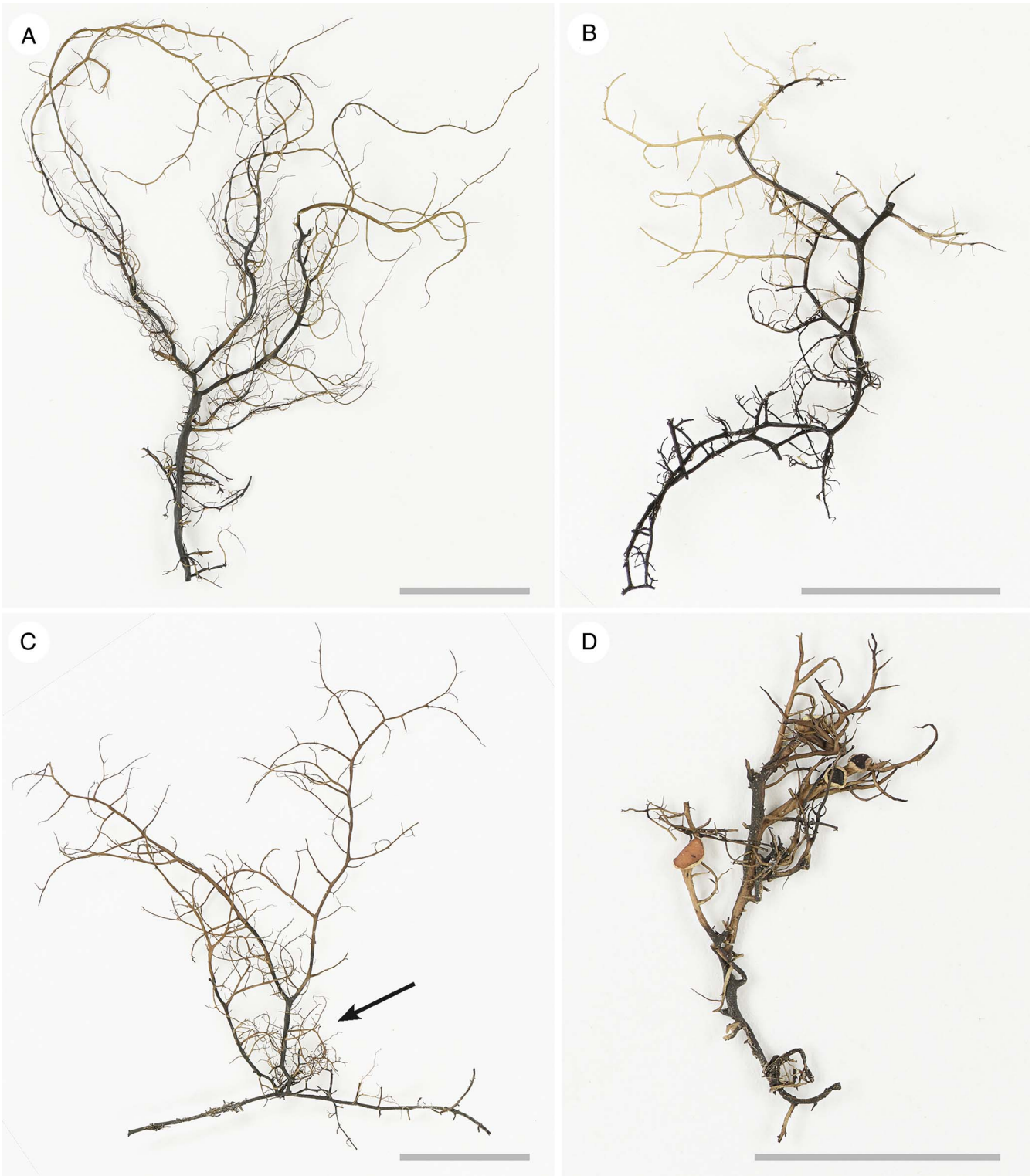

Figure 4. General habits of *Bryoria ahtiana* sp. nov., *B. bicolor*, *B. fruticulosa* and *B. yunnanensis*. A, *B. ahtiana* (H—isotype) with mostly widely divergent branches including thick, distinctly tapering main stems and short, stiff third-order branchlets. B, *B. bicolor* (*Kuusinen* 1063 & *Lampinen*) with perpendicular second- and third-order branches and branchlets. C, *B. fruticulosa* (*Wang* 13-38482) with often dense and twisted third-order branchlets (shown with arrow). D, *B. yunnanensis* (H—isotype) with apothecia and poorly developed tertiary branches. Scales = 1 cm.

Two of these morphotypes (threadlike-flexuose and threadlike-spinulose) accounted for 42 of the 62 specimens examined by us, notwithstanding that the holotype of *B. tenuis* s. str. matches with the thickening-spinulose morphotype (Fig. 5F). No clear correlation was noted between thallus morphology and mycobiont phylogeny, with cobwebby, thickening-spinulose, threadlike-flexuose and threadlike-spinulose forms cropping up within both *B. tenuis* s. str. and *B. tenuis* s. lat. (Fig. 2).

https://doi.org/10.1017/S0024282923000555 Published online by Cambridge University Press

https://doi.org/10.1017/S0024282923000555 Published online by Cambridge University Press

Table 4. Comparison of the distinguishing characters of the species in subclade II, section *Divaricatae*. Information is based on herbarium material (ALA, CANL, H, KUN, O, TUR, UBC, UAAH and UPS) and literature (Bystrek 1969; Jørgensen & Ryvarden 1970; Jørgensen 1972; Brodo & Hawksworth 1977; Wang & Harada 2001; Hawksworth & Coppins 2003; Kurokawa & Kashiwadani 2006; Jørgensen & Tønsberg 2010; Jørgensen *et al.* 2012; Wang *et al.* 2017; Singh *et al.* 2018).

Species	Colour	Growth form	Branching pattern	3rd-order branchlets	Pseudocyphellae	Soralia	Apothecia	Distribution	Chemistry
Bryoria ahtiana	bicolorous: basal parts black, upper part pale brown to chestnut brown	caespitose, up to 7 cm	anisotomic dichotomous, main stems and 2nd-order branches thickening, becoming long and flexuose	sparse to abundant, axils acute to perpendicular, mostly spinulose	rare, inconspicuous, elongate fusiform, plane to slightly depressed, brown, 0.3–1 mm long	absent	unknown	USA (Alaska), Russia (Komi Republic)	fumarprotocetraric acid or no substances
B. asiatica	not bicolorous, dark brown to blackish	pendent, up to 30 cm	isotomic dichotomous, main stems not distinctly thickened	sparse, axils acute, spinulose	absent	absent	rare, spores *c.* 4 µm × 8 µm	China, India, Japan	no substances detected
B. barbata	not bicolorous, chestnut brown	decumbent to subpendent, up to 10 (15) cm	anisotomic dichotomous, main stems not distinctly thickened	sparse, axils acute, spinulose	conspicuous, oblong to fusiform, plane to slightly raised, greyish white, 0.5–1 mm long	absent	present, spores *c.* 4 µm × 5 µm	China (Yunnan)	fumarprotocetraric acid
B. bicolor	bicolorous: basal parts black, apical parts and spinules grey	erect to caespitose, up to 7 cm	isotomic dichotomous, main stems not distinctly thickened	abundant, axils acute to perpendicular, spinulose	absent or scarce, inconspicuous, fusiform, plane to slightly raised, brown to brownish white, 0.1–0.3 mm long (but see Brodo & Hawksworth (1977): up to 3.5 mm long)	absent	rare, spores 6–9 µm × 4–6 µm	Europe, Africa, Asia, North and South America; suboceanic	fumarprotocetraric acid complex
B. fruticulosa	bicolorous: basal parts black, upper part chestnut brown to dark brown, 3rd-order branches yellowish green to fawn brown	erect to decumbent, up to 6 cm	anisotomic dichotomous, main stems not distinctly thickened, 2nd-order branches sparse	abundant near branch tips, axils perpendicular, spinulose often becoming curved and twisted (broom-like), fragile	rare, conspicuous, fissural, depressed, greyish white, 0.1–0.5 mm long	very rare, tuberculate, wider than branches	rare, ciliate when mature, spores 7–8 µm × 4–5 µm	China (Hengduan Mtn)	fumarprotocetraric acid

(*Continued*)

https://doi.org/10.1017/S0024282923000555 Published online by Cambridge University Press

Table 4. (*Continued*)

Species	Colour	Growth form	Branching pattern	3rd-order branchlets	Pseudocyphellae	Soralia	Apothecia	Distribution	Chemistry
B. rigida	bicolorous: basal parts black, apical parts olivaceous brown	erect, up to 5 cm	anisotomic dichotomous, main stems stiff, coarse, thickening inwards	abundant, axils mainly acute, spinulose	elongate fusiform, plane or slightly depressed, black, 0.2–0.7 mm long	absent	unknown	China, India	fumarprotocetraric acid complex
B. tenuis	bicolorous: basal parts black, apical parts pale brown to dark brown	mostly subpendent-pendent, up to 12 cm	variable (Fig. 5): mostly anisotomic-dichotomous, main stems uniformly thin or thickening inwards	sparse, axils acute to perpendicular, spinulose to long-flexuose	sparse to abundant, usually inconspicuous, fissural-fusiform, plane to slightly raised, white to dark, 0.1–0.8 mm long	absent	rare, spores 7–10 μm × 5–7 μm	*B. tenuis* s. str.: Europe, Asia, North America; oceanic *B. tenuis* s. lat.: North America: Canada (British Columbia), USA (Alaska); oceanic	fumarprotocetraric acid complex
B. yunnanensis	bicolorous: basal parts black, apical parts fawn brown to pale brown	decumbent to erect, up to 4 cm	mostly anisotomic dichotomous, main stems distinctly thickening inwards	sparse, axils perpendicular, spinulose	oblong-ellipsoid, depressed, greyish white 0.5 mm long	absent	present, spores 7–8 μm × 10–12 μm	China	fumarprotocetraric acid, trace of an unknown compound (C solvent: R_f 2–3, light green)

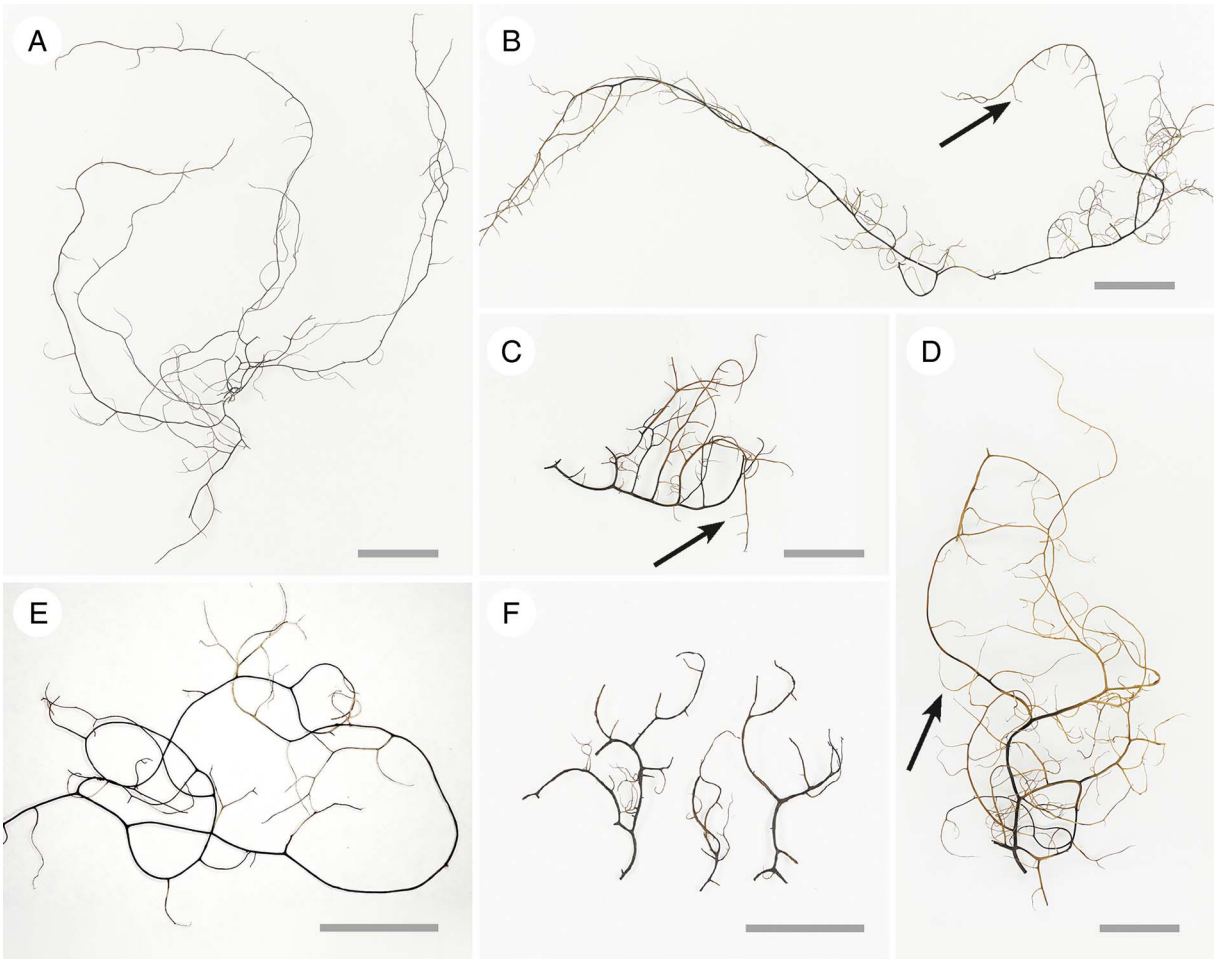

Figure 5. Thallus morphologies of *Bryoria tenuis*, see text. A, cobwebby (finely threadlike) (*B. tenuis* s. lat. L980, UBC). B, threadlike-spinulose with short and rather stiff third-order branchlets (arrow) (*B. tenuis* s. lat. L1038, H). C, thickening-spinulose with short and rather stiff third-order branchlets (arrow) (*B. tenuis* s. str. L164, UPS). D, thickening-flexuose with longer and more flexuous third-order branchlets (arrow) (*B. tenuis* s. lat. L879, H). E, threadlike-flexuose with weakly arcing terminal branches (*B. tenuis* ALA L034794). F, holotype of *B. tenuis* (O) representing the (rather brittle) thickening-spinulose morphotype. Scales = 1 cm.

Species delimitation in section Divaricatae

The results obtained from species delimitation analyses are summarized in Table 3. The ASAP method based on genetic distances gave the smallest number of putative species while the two GMYC threshold analyses yielded the highest number. In general, none of the methods was fully consistent with the current taxonomy as the majority of partitions containing at least two samples were comprised of specimens identified as different species. Samples clustered in subclades I and II in the six-locus phylogeny were separated in all analyses. In subclade II, *Bryoria tenuis* s. str. was determined as a single species in the bPTP analysis of the ITS data set. None of the analyses identified the combination *B. tenuis* s. str. and *B. tenuis* s. lat. as a single species. Furthermore, none of the analyses recognized the *B. tenuis* s. lat. clade from the ITS phylogeny as a separate partition. *Bryoria bicolor* was recognized as a single species only in the GMYC multiple threshold analysis of the ITS data set, and *B. rigida* in the ASAP analyses of the IGS and mtSSU data sets as well as the bPTP analyses of the ITS and IGS data sets. *Bryoria ahtiana* was inferred as a distinct species in the GMYC single threshold analysis of the *GAPDH* data set and in the GMYC multiple threshold analyses of the ITS and *GAPDH* data sets. *Bryoria fruticulosa* was determined as a separate partition in the GMYC analyses of *GAPDH* data sets and *B. yunnanenis* in the GMYC multiple threshold analysis of the mtSSU data set and the bPTP analysis of the ITS data set. *Bryoria asiatica* and *B. barbata* were both inferred as separate partitions in several analyses.

The marginal likelihood for the species hypotheses tested and the Bayes factor results are shown in Table 5. The model that considers 14 species (Hypothesis 1) with the current circumscription was the best supported, followed by the model that considers 13 species (Hypothesis 2), with *B. tenuis* and *B. tenuis* s. lat. forming a single species.

Discussion

Phylogeny of Bryoria

We used a six-locus dataset including three ribosomal (ITS, IGS, mtSSU) and three protein-coding markers (*GAPDH*, *Mcm7*, *Tsr1*) to examine infrageneric relationships in the genus *Bryoria* and to assess species delimitation in section *Divaricatae*. The addition of gene regions generally resulted in improved support values, especially for the backbone nodes. Our results confirm our previous findings (Myllys *et al.* 2014, 2016) that section *Bryoria sensu* Myllys *et al.* (2011) is polyphyletic and divides into two separate entities. *Bryoria* clade 1 was resolved as a sister group to *B.*

https://doi.org/10.1017/S0024282923000555 Published online by Cambridge University Press

Table 5. Evaluation of different species hypotheses using Bayes factor in section *Divaricatae*. SS = marginal likelihood calculated using stepping-stone sampling; PS = marginal likelihood calculated using path sampling; BF = Bayes factor. Hypotheses 1 & 2 follow the species concept used in this study and hypotheses 3–12 are obtained from species delimitation analyses. The model that considers 14 species (Hypothesis 1) with the current circumscription is the best supported, followed by the model that considers 13 species (Hypothesis 2).

Species delimitation hypotheses	SS	BF	PS	BF
1: current circumscription of the species: *Bryoria tenuis* and *B. tenuis* s. lat. separate species	−8960.4370	—	−9172.0952	—
2: current circumscription of the species but *B. tenuis* and *B. tenuis* s. lat. conspecific	−9637.9173	1355.9606	−9636.2059	928.2214
3: hypothesis generated by ASAP for ITS, *GAPDH*, *Mcm7* (2 species)	−9798.7139	1676.5538	−9796.8939	1249.5974
4: hypothesis generated by bPTP for *GAPDH* (3 species)	−9777.2602	1633.6464	−9775.7561	1207.3218
5: hypothesis generated by GMYC single for mtSSU (4 species)	−9719.5007	1518.1274	−9717.4803	1090.7702
6: hypothesis generated by bPTP for IGS (4 species)	−9743.9198	1566.9656	−9741.7484	1139.3064
7: hypothesis generated by bPTP for *Mcm7* (4 species)	−9757.0953	1593.3166	−9766.7260	1189.2616
8: hypothesis generated by ASAP for mtSSU (4 species)	−9706.8795	1492.885	−9706.2272	1068,264
9: hypothesis generated by PTP for mtSSU (5 species)	−9712.9526	1505.0312	−9710.9835	1077,7766
10: hypothesis generated by GMYC single for *GAPDH* (11 species)	−9639.5657	1358.2574	−9635.7433	927.2962
11: hypothesis generated by PTP for ITS (12 species)	−9659.9444	1.399,0148	−9657.2736	970.3568
12: hypothesis generated by GMYC multiple for *GAPDH* (13 species)	−9644.2052	1367.5364	−9640.6344	937.0784

americana and is placed here in an emended section *Americanae*. No morphological characters were found to support the separation of section *Bryoria* into two groups, but the distributions of the two clades clearly differ. In their new circumscription, section *Bryoria* consists mostly of species with broad discontinuously circumpolar distributions while section *Americanae*, with the exception of the widely distributed *B. americana*, is restricted to western North America and the Himalayan region.

Our six-locus phylogeny confirmed the circumscription of section *Divaricatae* as presented in Myllys *et al.* (2011). This is in contrast to the ITS + *Mcm7* phylogeny of Myllys *et al.* (2016) and the ITS phylogeny of Wang *et al.* (2017), both of which excluded *B. confusa*, *B. nepalensis*, *B. smithii*, *B. variabilis* and *B. wui* (corresponding to subclade I in the present study) from this section. The conflicting results are probably due to low backbone resolution in those two- and single locus phylogenies, as well as to the long branch leading to these species. All the species in this subclade lack secondary substances while most of the species in subclade II, namely *B. barbata*, *B. bicolor*, *B. fruticulosa*, *B. rigida*, *B. tenuis* (including *B. tenuis* s. lat.) and *B. yunnanensis*, contain fumarprotocetraric acid. In our earlier study (Myllys *et al.* 2011), we suggested that the section can be regarded as morphologically well defined insofar as all species have a characteristic bicolorous thallus with blackened basal parts and greyish brown to olive-brown apical branches that bear spinulose third-order branchlets (see Jørgensen & Ryvarden 1970; Jørgensen 1972, 1975; Brodo & Hawskworth 1977). However, contrary to our definition, Wang *et al.* (2017) noted that *B. barbata* and *B. wui* are uniform in colour, as had earlier been reported for *B. asiatica* (Wang & Harada 2001; see also Table 4). Furthermore, based on our inspection of *B. tenuis* s. str. and *B. tenuis* s. lat. (e.g. specimens *B. tenuis* L681 and *B. tenuis* s. lat. L693), the colour difference between the basal and apical portions is not always clear since the latter are medium brown rather than pale brown. The differences in colour within these taxa are probably the result of differing ecological conditions and of no taxonomic significance. Furthermore, in some material of *B. tenuis* s. lat. specimens, pale and black parts are not always restricted to apical and basal parts but alternate on main branches (e.g. in specimens L225, L696 and L980).

Brodo & Hawksworth (1977) suggested that *Divaricatae* is an evolutionary ancient group but recent molecular phylogenies (Myllys *et al.* 2016; Wang *et al.* 2017) including this study (Fig. 3) show that this section is of recent origin and is currently undergoing diversification, especially in South-East Asia but also in western North America (Jørgensen *et al.* 2012; Myllys *et al.* 2016; Wang *et al.* 2017; McCune *et al.* 2020). High speciation rates have previously been reported in several *Parmeliaceae* taxa, including *Bryoria* section *Implexae* (Boluda *et al.* 2019) and *Usnea* (Kraichak *et al.* 2015; Mark *et al.* 2016).

Our dating results are congruent with those of Boluda *et al.* (2019) but younger than those presented by Divakar *et al.* (2017), probably an artefact of different methodologies. While we followed Boluda *et al.* (2019) and used the *Melanohalea* substitution rate (Leavitt *et al.* 2012), Divakar *et al.* (2017) used secondary calibrations based on a fossil-dated phylogeny (Amo de Paz *et al.* 2011). However, as pointed out by Graur & Martin (2004), secondary calibration based on a single calibration point can produce errors. The origin of *Bryoria* coincides with the period of global cooling that occurred until the early Pliocene (Zachos *et al.* 2001). This indicates that the diversification of the main *Bryoria* groups occurred in a cold period dominated by coniferous forests (Sanmartín *et al.* 2001).

Species delimitation in section Divaricatae

Whereas the topologies of our phylogenetic trees from ITS and IGS were mostly congruent and supported current species concepts in section *Divaricatae*, the remaining gene regions were less informative and produced more poorly resolved and partly conflicting phylogenetic trees (Fig. 2) and highly inconsistent species delimitation. We suggest that the lack of species monophyly in analyses of these latter loci, as well as the non-congruence of the species delimitation results, are related to the recent

https://doi.org/10.1017/S0024282923000555 Published online by Cambridge University Press

divergence of the species. A similar case has been reported in the *B. fuscescens* complex (Boluda *et al.* 2019), where lack of genetic differentiation between the species is attributed to their recent divergence *c.* 1 Mya. Further similar cases have also been observed in other groups (McMullin *et al.* 2016; Pino-Bodas *et al.* 2018; Jorna *et al.* 2021; Asher *et al.* 2023), highlighting the difficulty of species delimitation in recently evolved groups with complex, recent phylogeographical histories.

Inconsistencies between different species delimitation methods have been widely discussed in the literature. In some cases, these may reflect a violation of the foundational assumptions of the methods (Carstens *et al.* 2013), while in others they may result from biases arising from the number of per-species haplotypes being analyzed, the geographical distance between intraspecific sampling locations, or the taxonomic range analyzed (Lohse 2009; Ahrens *et al.* 2016; Sukumaran & Knowles 2017; Hofmann *et al.* 2019; Magoga *et al.* 2021). Such inconsistencies led Carstens *et al.* (2013) to recommend an integrative taxonomy approach in which the results of several different species delimitation methods are compared with phenotypic and ecological data and distribution patterns (Dayrat 2005; Maharachchikumbura *et al.* 2021) before taxonomic changes are introduced.

Incongruences among gene regions may also be linked to biological causes such as recombination, hybridization and incomplete lineage sorting. In the present case, we consider the last explanation most likely in the predominantly sterile species *B. bicolor* and *B. tenuis*, whereas recombination and hybridization may play a role in *B. fruticulosa* and *B. yunnanensis*, both of which regularly produce apothecia. Hybridization has been detected in other genera in the *Parmeliaceae*, most recently in *Xanthoparmelia* (Keuler *et al.* 2022). Incongruent results obtained from the *Mcm7* gene may also reflect gene duplication and paralog formation as shown in *Usnea* (Lücking *et al.* 2020).

Inclusion of additional markers may either support the topology obtained from a single marker or increase resolution where a single marker such as ITS is not sufficient to provide adequate resolution to assess species boundaries (Lücking *et al.* 2021). In the present study, however, the addition of other gene regions traditionally used in phylogenetic studies did not always increase phylogenetic resolution in section *Divaricatae*. Thus, in the ITS phylogeny both *B. tenuis* and *B. tenuis* s. lat. were resolved as monophyletic lineages, while in the multi-locus phylogeny, the *B. tenuis* clade was not resolved as monophyletic but grouped with *B. tenuis* s. lat. While *B. tenuis* s. str. was strongly supported in all analyses obtained from ITS data, the emended lineage in the multi-locus tree was strongly supported only in the Bayesian analysis. Furthermore, in the parsimony tree obtained from the combined data set (Supplementary Materials Fig. S1, available online), neither *B. bicolor* nor *B. tenuis* s. str. were resolved as monophyletic but appeared in a strongly supported, largely unresolved group with *B. ahtiana*, *B. fruticulosa*, *B. tenuis* s. lat. and *B. yunnanensis*, suggesting that all these taxa should be treated as conspecific. These results highlight the difficulty in separating closely related species using multi-locus approaches and illustrate that decisions regarding conspecificity should be made with caution (see Grewe *et al.* 2018).

According to current knowledge, most *Bryoria* species in section *Divaricatae* can be regarded as morphologically rather conservative, varying within a relatively narrow range of thallus morphologies. A notable exception is *B. tenuis* which, as circumscribed here, appears to be a highly morphologically plastic species (Fig. 5). Rather unexpectedly, both *B. tenuis* s. str. and *B. tenuis* s. lat. produce all five morphologies, which thus occur throughout the range of the species as a whole; however, whether they are under some form of genetic control or represent variation in ecotypic response is unknown. Initially we intended to recognize *Bryoria tenuis* s. lat. as a distinct species recently diverged from *B. tenuis* s. str., a treatment consistent with our ITS data and Bayes factor results, and further supported by its strictly western North American distribution (versus the more or less circumpolar-oceanic distribution of *B. tenuis* s. str.). Given, however, the lack of corroborating morphological evidence outlined in the present study, we feel that species recognition, if warranted at all, must await further study, including information on the identity of the photobionts. In the future, genome-scale data will potentially be useful in addressing species delimitation in *Bryoria*. RADseq approaches in particular have provided sufficient resolution to separate recently diverged species, including the species pair *Usnea antarctica*/*U. aurantiacoatra* (Grewe *et al.* 2018), the *Rhizoplaca melanophthalma* complex (Grewe *et al.* 2017) and *Pseudocyphellaria* (Widhelm *et al.* 2023). Furthermore, species partitions inferred from ITS in the genus *Niebla* Rundel & Bowler (*Ramalinaceae*) have been shown to coincide with clades inferred from RADseq markers (Jorna *et al.* 2021).

Taxonomy

Bryoria ahtiana Myllys & Goward sp. nov.

MycoBank No.: MB 848936

Thallus hairlike, bicolorous with basal parts black and apical parts brown, branching predominantly anisotomic, main stems distinctly thick, gradually tapering towards tips, with few to many stiff, spinulose third-order branchlets; resembling *B. tenuis* but with thicker, more distinctly tapering main stems and shorter, stiffer third-order branchlets. Epiphytic or saxicolous.

Type: USA, Alaska, Kenai Peninsula Borough, Kenai Fjords National Park, N end of Harris Bay, near opening to Northwestern Lagoon, open alluvial flats with groves of young *Picea*, elevation 3 m, 59.7487°N, 149.8462°W, NAD83, on *Picea* snag, 8 July 2015, *Bruce McCune* et al. 36219 (OSC—holotype; H—isotype, H9214302). GenBank Accession nos: MN906272 (ITS), OR060816 (IGS).

(Fig. 4A)

Thallus caespitose, hair-like, up to 7 cm long, bicolorous, basal portions black, apical portions pale brown to chestnut brown. *Branching* anisotomic, giving rise to distinct, conspicuously thickened main stems and sparse secondary branches, main stems to 3 cm long and 0.7 mm wide, terminal portions mostly long and flexuous, rather shiny. *Third-order branchlets* sparse to abundant, mostly perpendicular, and spinulose; *spinules* 1–4 mm long. *Pseudocyphellae* rare, inconspicuous, brownish dark brown, elongate fusiform, plane or slightly depressed, *c.* 0.05 mm wide, 0.3–1 mm long. *Soralia* and *isidia* absent.

Apothecia and *condiomata* not seen.

Chemistry. Cortex and medulla Pd− or Pd+ red, secondary substances absent or containing fumarprotocetraric acid.

Etymology. Named in honour of Prof. Teuvo Ahti, the Finnish lichenologist, in recognition of his long interest in and

https://doi.org/10.1017/S0024282923000555 Published online by Cambridge University Press

outstanding contributions to lichenology in western North America, both through his taxonomic research (e.g. Ahti & Henssen 1965; Goward & Ahti 1983, 1997; Brodo & Ahti 1996; Ahti 2007) and his unstinting willingness to help and encourage up-and-coming lichenologists in the region.

Distribution and habitat. The new species is currently known from two specimens: one from Alaska, USA in the oceanic boreal region, and one from the Komi Republic of Russia in the low alpine.

Notes. *Bryoria ahtiana* is a non-sorediate hair lichen distinguished by its bicolorous, widely divergent thallus, conspicuously thickened main stems, well-developed secondary branches, and typically sparse third-order branchlets. It may be confused with the closely related *B. tenuis*, which is, however, more pendent and has thinner, less conspicuous main stems, usually with more numerous third-order branchlets. Also closely related are the bicolorous species *B. bicolor*, *B. fruticulosa*, *B. rigida* and *B. yunnanensis*, all of which differ from *B. ahtiana* in their habit and branching pattern: *B. bicolor* is erect to caespitose and has perpendicular second- and third-order branches and branchlets; *B. fruticulosa*, with usually sparse second-order branches, is erect to decumbent and has dense, fragile third-order branchlets; *B. rigida* is erect and has a stiff, coarse habit and short third-order branchlets; and *B. yunnanensis* is a small, often erect, usually fertile species with sparse third-order branchlets (Fig. 4, Table 4). While *B. ahtiana* is sympatric with *B. bicolor* in north-west North America, *B. fruticulosa*, *B. rigida* and *B. yunnanensis* are known only from South-East Asia (Jørgensen *et al.* 2012; Wang *et al.* 2017).

Fumarprotocetraric acid could not be detected in the type specimen, although this substance was present in small amounts in the Komi specimen (L168); this is consistent with Brodo & Hawksworth (1977), who reported that fumarprotocetraric acid in *B. tenuis* may be localized or present in low concentrations, and therefore easily overlooked in routine testing.

Additional specimen examined. **Russia:** *Komi Republic*: Troitsko-Pechorskii, Hrebet Ebel´Is, N slope and top, 21.5 km NW of Ust-Ljaga, saxicolous on small slate rocks at low alpine subzone, 600–720 m, 62°38′N, 58°45′E, 9 vi 2003, *J. O. Hermansson* 12625 (UPS L-132835).

Acknowledgements. We thank Emilia Piki, Emelie Winquist and Marijke Iso-Kokkila for help with laboratory work, Tuomas Kuusinen for technical assistance, Leena Helynranta for preparing Figs 4 and 5, Bruce McCune and Sarah Jovan for arranging fresh material, and Karen Dillman for kindly providing collection information for her specimens. We also thank two reviewers for their helpful comments on the manuscript and the curators of herbaria ALA, CANL, KUN, O, TUR, UAAH, UBC and UPS for providing material. The study was financially supported by the Academy of Finland (grant 323711 to LM). RPB was funded by the Talent Attraction program (ref. 2020-T1/AMB-19852, Comunidad de Madrid).

Author ORCIDs. Leena Myllys, 0000-0002-9566-9473; Raquel Pino-Bodas, 0000-0001-5228-5368; Saara Velmala, 0000-0002-9386-243X; Li-Song Wang, 0000-0003-3721-5956; Trevor Goward, 0000-0003-2655-9956.

Competing Interests. The authors declare none.

Supplementary Material. The Supplementary Material for this article can be found at https://doi.org/10.1017/S0024282923000555.

References

Ahrens D, Fujisawa T, Krammer HJ, Eberle J, Fabrizi S and Vogler AP (2016) Rarity and incomplete sampling in DNA-based species delimitation. *Systematic Biology* **65**, 478–494.

Ahti T (2007) Further studies on the *Cladonia verticillata* group (*Lecanorales*) in East Asia and western North America. *Bibliotheca Lichenologica* **96**, 5–19.

Ahti T and Henssen A (1965) New localities for *Cavernularia hultenii* in eastern and western North America. *Bryologist* **68**, 85–89.

Amo de Paz G, Cubas P, Divakar PK, Lumbsch HT and Crespo A (2011) Origin and diversification of major clades in parmelioid lichens (*Parmeliaceae*, *Ascomycota*) during the Paleogene inferred by Bayesian analysis. *PLoS ONE* **6**, e28161.

Asher OA, Howieson J and Lendemer JC (2023) A new perspective on the macrolichen genus *Platismatia* (*Parmeliaceae*, *Ascomycota*) based on molecular and phenotypic data. *Bryologist* **126**, 1–18.

Boluda CG, Divakar PK, Hawksworth DL, Villagra J and Rico VJ (2015) Molecular studies reveal a new species of *Bryoria* in Chile. *Lichenologist* **47**, 387–394.

Boluda CG, Rico VJ, Divakar PK, Nadyeina O, Myllys L, McMullin RT, Zamora JC, Scheidegger C and Hawksworth DL (2019) Evaluating methodologies for species delimitation: the mismatch between phenotypes and genotypes in lichenized fungi (*Bryoria* sect. *Implexae, Parmeliaceae*). *Persoonia* **42**, 75–100.

Brodo IM and Ahti T (1996) Lichens and lichenicolous fungi of the Queen Charlotte Islands, British Columbia, Canada. 2. The *Cladoniaceae*. *Canadian Journal of Botany* **74**, 1147–1180.

Brodo IM and Hawksworth DL (1977) *Alectoria* and allied genera in North America. *Opera Botanica* **42**, 1–164.

Bystrek J (1969) Die Gattung *Alectoria*. *Lichenes*, *Usneaceae* (Flechten des Himalaya 5). *Khumbu Himal* **6**, 17–24.

Carstens BC, Pelletier TA, Reid NM and Satler JD (2013) How to fail at species delimitation. *Molecular Ecology* **22**, 4369–4383.

Dayrat B (2005) Towards integrative taxonomy. *Biological Journal of the Linnean Society* **85**, 407–417.

Divakar PK, Crespo A, Wedin M, Leavitt S, Hawksworth D, Myllys L, McCune B, Randlane T, Bjerke JW, Ohmura Y, *et al.* (2015) Evolution of complex symbiotic relationships in a morphologically derived family of lichen-forming fungi. *New Phytologist* **208**, 1217–1226.

Divakar PK, Crespo A, Kraichak E, Leavitt SD, Singh G, Schmitt I and Lumbsch HT (2017) Using a temporal phylogenetic method to harmonize family- and genus-level classification in the largest clade of lichen-forming fungi. *Fungal Diversity* **84**, 101–117.

Drummond AJ, Suchard MA, Xie D and Rambaut A (2012) Bayesian phylogenetics with BEAUti and the BEAST 1.7. *Molecular Biology and Evolution* **29**, 1969–1973.

Edgar RC (2004) MUSCLE: multiple sequence alignment with high accuracy and high throughput. *Nucleic Acids Research* **32**, 1792–1797.

Fontaine KM, Ahti T and Piercey-Normore MD (2010) Convergent evolution in *Cladonia gracilis* and allies. *Lichenologist* **42**, 1–16.

Fujisawa T and Barraclough TG (2013) Delimiting species using single-locus data and the Generalized Mixed Yule Coalescent approach: a revised method and evaluation on simulated data sets. *Systematic Biology* **62**, 707–724.

Gardes M and Bruns TD (1993) ITS primers with enhanced specificity for basidiomycetes – application to the identification of mycorrhizae and rusts. *Molecular Ecology* **2**, 113–118.

Gargas A and Taylor JW (1992) Polymerase chain reaction (PCR) primers for amplifying and sequencing nuclear 18S rDNA from lichenized fungi. *Mycologia* **84**, 589–592.

Goloboff PA, Farris JS and Nixon KC (2008) TNT, a free program for phylogenetic analysis. *Cladistics* **24**, 774–786.

Goward T and Ahti T (1983) *Parmelia hygrophila*, a new lichen species from the Pacific Northwest of North America. *Bryologist* **20**, 9–13.

Goward T and Ahti T (1997) Notes on the distributional ecology of the *Cladoniaceae* (lichenized *Ascomycetes*) in temperate and boreal western North America. *Journal of the Hattori Botanical Laboratory* **82**, 143–155.

Goward T, Gauslaa Y, Björk CR, Woods D and Wright KG (2022) Stand openness predicts hair lichen (*Bryoria*) abundance in the lower canopy, with implications for the conservation of Canada's critically imperiled Deep-Snow Mountain Caribou (*Rangifer tarandus caribou*). *Forest Ecology and Management* **520**, 120416.

Graur D and Martin W (2004) Reading the entrails of chickens: molecular timescales of evolution and the illusion of precision. *Trends in Genetics* **20**, 80–86.

Grewe F, Huang JP, Leavitt SD and Lumbsch HT (2017) Reference-based RADseq resolves robust relationships among closely related species of lichen-forming fungi using metagenomic DNA. *Scientific Reports* **7**, 1–11.

Grewe F, Lagostina E, Wu H, Printzen C and Lumbsch HT (2018) Population genomic analyses of RAD sequences resolves the phylogenetic relationship of the lichen-forming fungal species *Usnea antarctica* and *Usnea aurantiacoatra*. *MycoKeys* **43**, 61–113.

Hawksworth DL and Coppins BJ (2003) *Bryoria tenuis* (*Parmeliaceae*) new to the British Isles, and either awaiting rediscovery or extinct. *Lichenologist* **35**, 361–364.

Heled J and Drummond AJ (2010) Bayesian inference of species trees from multilocus data. *Molecular Biology and Evolution* **27**, 570–580.

Hofmann EP, Nicholson KE, Luque-Montes IR, Köhler G, Cerrato-Mendoza CA, Medina-Flores M, Wilson LD and Townsend JH (2019) Cryptic diversity, but to what extent? Discordance between single-locus species delimitation methods within mainland anoles (*Squamata*: *Dactyloidae*) of northern Central America. *Frontiers in Genetics* **10**, 11.

Jørgensen PM (1972) Further studies in *Alectoria* sect. *Divaricatae* DR. *Svensk Botanisk Tidskrift* **66**, 191–201.

Jørgensen PM (1975) Further notes on Asian *Alectoria*. *Bryologist* **78**, 77–80.

Jørgensen PM and Ryvarden L (1970) Contribution to the lichen flora of Norway. *Årbok for Universitetet I Bergen, Matematisk-Naturvidenskapelig Serie* 1969 **10**, 1–24.

Jørgensen PM and Tønsberg T (2010) The lichen *Bryoria bicolor* found fertile in western Norway. *Graphis Scripta* **22**, 52–53.

Jørgensen PM, Myllys L, Velmala S and Wang LS (2012) *Bryoria rigida*, a new Asian lichen species from the Himalayan region. *Lichenologist* **44**, 777–781.

Jorna J, Linde JB, Searle PC, Jackson AC, Nielsen M-E, Nate MS, Saxton NA, Grewe F, Herrera-Campos MA, Spjut RW, *et al.* (2021) Species boundaries in the messy middle – a genome-scale validation of species delimitation in a recently diverged lineage of coastal fog desert lichen fungi. *Ecology and Evolution* **11**, 18615–18632.

Keuler R, Jensen J, Barcena-Peña A, Grewe F, Lumbsch HT, Huang JP and Leavitt SD (2022) Interpreting phylogenetic conflict: hybridization in the most speciose genus of lichen-forming fungi. *Molecular Phylogenetics and Evolution* **174**, 107543.

Kotelko R and Piercey-Normore MD (2010) *Cladonia pyxidata* and *C. pocillum*; genetic evidence to regard them as conspecific. *Mycologia* **102**, 534–545.

Kraichak E, Divakar PK, Crespo A, Leavitt SD, Nelsen MP, Lücking R and Lumbsch HT (2015) A tale of two hyper-diversities: diversification dynamics of the two largest families of lichenized fungi. *Scientific Reports* **5**, 10028.

Kurokawa S and Kashiwadani H (2006) *Checklist of Japanese Lichens and Allied Fungi*. Tokyo: National Science Museum.

Leavitt SD, Johnson L and St Clair LL (2011) Species delimitation and evolution in morphologically and chemically diverse communities of the lichen-forming genus *Xanthoparmelia* (*Parmeliaceae*, *Ascomycota*) in western North America. *American Journal of Botany* **98**, 175–188.

Leavitt SD, Esslinger TL, Divakar PK and Lumbsch HT (2012) Miocene and Pliocene dominated diversification of the lichen-forming fungal genus *Melanohalea* (*Parmeliaceae*, *Ascomycota*) and Pleistocene population expansions. *BMC Evolutionary Biology* **12**, 1–18.

Leavitt SD, Esslinger TL, Divakar PK, Crespo A and Lumbsch HT (2016) Hidden diversity before our eyes: delimiting and describing cryptic lichen-forming fungal species in camouflage lichens (*Parmeliaeceae*, *Ascomycota*). *Fungal Biology* **120**, 1374–1391.

Lohse K (2009) Can mtDNA barcodes be used to delimit species? A response to Pons et al. (2006). *Systematic Biology* **58**, 439–442.

Lohtander K, Myllys L, Sundin R, Källersjö M and Tehler A (1998) The species pair concept in the lichen *Dendrographa leucophaea* (*Arthoniales*): analyses based on ITS sequences. *Bryologist* **101**, 404–411.

Lohtander K, Oksanen I and Rikkinen J (2002) A phylogenetic study of *Nephroma* (lichen-forming *Ascomycota*). *Mycological Research* **106**, 777–787.

Lücking R, Nadel MRA, Araujo E and Gerlach A (2020) Two decades of DNA barcoding in the genus *Usnea* (*Parmeliaceae*): how useful and reliable is the ITS? *Plant and Fungal Systematics* **65**, 303–357.

Lücking R, Leavitt SD and Hawksworth DL (2021) Species in lichen-forming fungi: balancing between conceptual and practical considerations, and between phenotype and phylogenomics. *Fungal Diversity* **109**, 99–154.

Lumbsch HT and Leavitt SD (2011) Goodbye morphology? A paradigm shift in the delimitation of species in lichenized fungi. *Fungal Diversity* **50**, 59–72.

Lutsak T, Fernández-Mendoza F, Kirika P, Wondafrash M and Printzen C (2020) Coalescence-based species delimitation using genome-wide data reveals hidden diversity in a cosmopolitan group of lichens. *Organisms Diversity and Evolution* **20**, 189–218.

Magoga G, Fontaneto D and Montagna M (2021) Factors affecting the efficiency of molecular species delimitation in a species-rich insect family. *Molecular Ecology Resources* **21**, 1475–1489.

Maharachchikumbura SS, Chen Y, Ariyawansa HA, Hyde KD, Haelewaters D, Perera RH, Samarakoon MC, Wanasinghe DN, Bustamante DE, Liu J-J, *et al.* (2021) Integrative approaches for species delimitation in *Ascomycota*. *Fungal Diversity* **109**, 155–179.

Mark K, Saag L, Leavitt SD, Will-Wolf S, Nelsen MP, Tõrra T, Saag A, Randlane T and Lumbsch HT (2016) Evaluation of traditionally circumscribed species in the lichen-forming genus *Usnea*, section *Usnea* (*Parmeliaceae*, *Ascomycota*) using a six-locus dataset. *Organisms Diversity and Evolution* **16**, 497–524.

McCune B, Arup U, Breuss O, Di Meglio E, Di Meglio J, Esslinger TL, Miadlikowska J, Miller AE, Rosentreter R, Schultz M, *et al.* (2020) Biodiversity and ecology of lichens of Kenai Fjords National Park, Alaska. *Plant and Fungal Systematics* **65**, 586–619.

McMullin RT, Lendemer JC, Braid HE and Newmaster SG (2016) Molecular insights into the lichen genus *Alectoria* (*Parmeliaceae*) in North America. *Botany* **94**, 165–175.

Miller MA, Pfeiffer W and Schwartz T (2010) Creating the CIPRES Science Gateway for inference of large phylogenetic trees. In *Proceedings of the Gateway Computing Environments Workshop* (*GCE*), 14 *November* 2010, *New Orleans, Louisiana*, pp. 1–8.

Myllys L, Lohtander K, Källersjö M and Tehler A (1999) Sequence insertions and ITS data provide congruent information on *Roccella canariensis* and *R. tuberculata* (*Arthoniales, Euascomycetes*) phylogeny. *Molecular Phylogenetics and Evolution* **12**, 295–309.

Myllys L, Stenroos S and Thell A (2002) New genes for phylogenetic studies of lichenized fungi: glyceraldehyde-3-phosphate dehydrogenase and beta-tubulin genes. *Lichenologist* **34**, 237–246.

Myllys L, Velmala S, Holien H, Halonen P, Wang LS and Goward T (2011) Phylogeny of the genus *Bryoria*. *Lichenologist* **45**, 617–638.

Myllys L, Velmala S, Lindgren H, Glavich D, Carlberg T, Wang LS and Goward T (2014) Taxonomic delimitation of the genera *Bryoria* and *Sulcaria*, with a new combination *Sulcaria spiralifera* introduced. *Lichenologist* **46**, 737–752.

Myllys L, Velmala S, Pino-Bodas R and Goward T (2016) New species in *Bryoria* (*Parmeliaceae*, *Lecanoromycetes*) from north-west North America. *Lichenologist* **48**, 355–365.

Orange A, James PW and White FJ (2001) *Microchemical Methods for the Identification of Lichens*. London: British Lichen Society.

Padial JM, Castroviejo-Fisher S, Koehler J, Vila C, Chaparro JC and De la Riva I (2009) Deciphering the products of evolution at the species level: the need for an integrative taxonomy. *Zoologica Scripta* **38**, 431–447.

Paradis E, Claude J and Strimmer K (2004) APE: analyses of phylogenetics and evolution in R language. *Bioinformatics* **20**, 289–290.

Piercey-Normore MD, Ahti T and Goward T (2010) Phylogenetic and haplotype analyses of four segregates within *Cladonia arbuscula* s.l. *Botany* **88**, 397–408.

Pino-Bodas R, Burgaz AR, Martín MP and Lumbsch HT (2011) Phenotypical plasticity and homoplasy complicate species delimitation in the *Cladonia gracilis* group (*Cladoniaceae*, *Ascomycota*). *Organisms Diversity and Evolution* **11**, 343–355.

Pino-Bodas R, Burgaz AR, Martín MP, Ahti T, Stenroos S, Wedin M and Lumbsch HT (2015) The phenotypic features used for distinguishing species within the *Cladonia furcata* complex are highly homoplasious. *Lichenologist* **47**, 287–303.

Pino-Bodas R, Burgaz AR, Ahti T and Stenroos S (2018) Taxonomy of *Cladonia angustiloba* and related species. *Lichenologist* **50**, 267–282.

https://doi.org/10.1017/S0024282923000555 Published online by Cambridge University Press

Pons J, Barraclough TG, Gomez-Zurita J, Cardoso A, Duran DP, Hazell S, Kamoun S, Sumlin WD and Vogler AP (2006) Sequence-based species delimitation for the DNA taxonomy of undescribed insects. *Systematic Biology* **55**, 595–609.

Posada D (2008) jModelTest: phylogenetic model averaging. *Molecular Biology and Evolution* **25**, 1253–1256.

Printzen C and Ekman S (2002) Genetic variability and its geographical distribution in the widely disjunct *Cavernularia hultenii*. *Lichenologist* **34**, 101–111.

Puillandre N, Brouillet S and Achaz G (2021) ASAP: assemble species by automatic partitioning. *Molecular Ecology Resources* **21**, 609–620.

Rambaut A and Drummond AJ (2013) *TreeAnnotator v. 1.7.0*. Available as part of the BEAST package [WWW resource] URL http://beast.bio.ed.ac.uk.

Rambaut A, Drummond AJ, Xie D, Baele G and Suchard MA (2018) Posterior summarization in Bayesian phylogenetics using Tracer 1.7. *Systematic Biology* **67**, 901–904.

Randlane T and Mark K (2021) Response to Clerc & Naciri (2021) *Usnea dasopoga* (Ach.) Nyl. and *U. barbata* (L.) F. H. Wigg. (*Ascomycetes*, *Parmeliaceae*) are two different species: a plea for reliable identifications in molecular studies. *Lichenologist* **53**, 231–232.

Ronquist F, Teslenko M, van der Mark P, Ayres DL, Darling A, Höhna S, Larget B, Liu L, Suchard MA and Huelsenbeck JP (2012) MrBayes 3.2: efficient Bayesian phylogenetic inference and model choice across a large model space. *Systematic Biology* **61**, 539–542.

Sanmartín I, Enghoff H and Ronquist F (2001) Patterns of animal dispersal, vicariance and diversification in the Holarctic. *Biological Journal of the Linnean Society* **73**, 345–390.

Schmitt I, Crespo A, Divakar PK, Fankhauser JD, Herman-Sackett E, Kalb K, Nelsen MP, Nelson NA, Rivas-Plata E, Shimp AD, *et al.* (2009) New primers for promising single-copy genes in fungal phylogenetics and systematics. *Persoonia* **23**, 35–40.

Schoch CL, Seifert KA, Huhndorf S, Robert V, Spouge JL, Levesque CA, Chen W and Fungal Barcoding Consortium (2012) Nuclear ribosomal internal transcribed spacer (ITS) region as a universal DNA barcode marker for Fungi. *Proceedings of the National Academy of Sciences of the United States of America* **109**, 6241–6246.

Singh KP, Singh P and Sinha GP (2018) Lichen diversity in the Eastern Himalaya biodiversity hotspot region, India. *Cryptogam Biodiversity and Assessment* Special Volume **2018**, 71–114.

Spribille T, Tuovinen V, Resl P, Vanderpool D, Wolinski H, Aime MC, Schneider K, Tabentheiner E, Toome-Heller M, Thor G, *et al.* (2016) Basidiomycete yeasts in the cortex of ascomycete macrolichens. *Science* **353**, 488–492.

Stamatakis A (2014) RAxML version 8: a tool for phylogenetic analysis and post-analysis of large phylogenies. *Bioinformatics* **30**, 1312–1313.

Sukumaran J and Knowles LL (2017) Multispecies coalescent delimits structure, not species. *Proceedings of the National Academy of Sciences of the United States of America* **114**, 1607–1612.

Thell A, Crespo A, Divakar PK, Kärnefelt I, Leavitt SD, Lumbsch HT and Seaward MRD (2012) A review of the family *Parmeliaceae* – history, phylogeny and current taxonomy. *Nordic Journal of Botany* **30**, 641–664.

Velmala S, Myllys L, Halonen P, Goward T and Ahti T (2009) Molecular data show that *Bryoria fremontii* and *B. tortuosa* (*Parmeliaceae*) are conspecific. *Lichenologist* **41**, 231–242.

Velmala S, Myllys L, Goward T, Holien H and Halonen P (2014) Taxonomy of *Bryoria* section *Implexae* (*Parmeliaceae*, *Lecanorales*) in North America and Europe, based on chemical, morphological and molecular data. *Annales Botanici Fennici* **51**, 345–371.

Wang LS and Harada H (2001) Taxonomic study of *Bryoria asiatica*-group (lichenized *Ascomycota*, *Parmeliaceae*) in Yunnan, southern China. *Natural History Research* **6**, 43–52.

Wang LS, Wang XY, Liu D, Myllys L, Shi HX, Zhang YY, Yang MX and Li LJ (2017) Four new species of *Bryoria* (lichenized *Ascomycota*: *Parmeliaceae*) from the Hengduan Mountains, China. *Phytotaxa* **297**, 29–41.

White TJ, Bruns TD, Lee SB and Taylor JW (1990) Amplification and direct sequencing of fungal ribosomal DNA genes for phylogenetics. In Innis MA, Gelfand DH, Sninsky JJ and White TJ (eds), *PCR Protocols: a Guide to Methods and Applications*. San Diego: Academic Press, pp. 315–322.

Widhelm TJ, Egan RS, Bertoletti FR, Asztalos MJ, Kraichak E, Leavitt SD and Lumbsch HT (2016) Picking holes in traditional species delimitations: an integrative taxonomic reassessment of the *Parmotrema perforatum* group (*Parmeliaceae*, *Ascomycota*). *Botanical Journal of the Linnean Society* **182**, 868–884.

Widhelm TJ, Rao A, Grewe F and Lumbsch HT (2023) High-throughput sequencing confirms the boundary between traditionally considered species pairs in a group of lichenized fungi (*Peltigeraceae*, *Pseudocyphellaria*). *Botanical Journal of the Linnean Society* **201**, 471–482.

Wiens JJ (2006) Missing data and the design of phylogenetic analyses. *Journal of Biomedical Informatics* **39**, 34–42.

Will KW, Mishler BD and Wheeler QD (2005) The perils of DNA barcoding and the need for integrative taxonomy. *Systematic Biology* **54**, 844–851.

Wirtz N, Printzen C and Lumbsch HT (2008) The delimitation of Antarctic and bipolar species of neuropogonoid *Usnea* (*Ascomycota*, *Lecanorales*): a cohesion approach of species recognition for the *Usnea perpusilla* complex. *Mycological Research* **112**, 472–484.

Zachos J, Pagani M, Sloan L, Thomas E and Billups K (2001) Trends, rhythms, and aberrations in global climate 65 Ma to present. *Science* **292**, 686–693.

Zhang J, Kapli P, Pavlidis P and Stamatakis A (2013) A general species delimitation method with applications to phylogenetic placements. *Bioinformatics* **29**, 2869–2876.

Zhao X, Fernández-Brime S, Wedin M, Locke M, Leavitt SD and Lumbsch HT (2017) Using multi-locus sequence data for addressing species boundaries in commonly accepted lichen-forming fungal species. *Organisms Diversity and Evolution* **17**, 351–363.

Zoller S, Scheidegger C and Sperisen C (1999) PCR primers for the amplification of mitochondrial small subunit ribosomal DNA of lichen-forming ascomycetes. *Lichenologist* **31**, 511–516.

https://doi.org/10.1017/S0024282923000555 Published online by Cambridge University Press